ACTRIS – Aerosols, Clouds and Trace gases Research Infrastructure
(www.actris.eu)

EARLINET – European Aerosol Research Lidar NETwork
(www.earlinet.org)

EARLINET/ACTRIS analysis of aerosol profiles during the COVID-19 lock-down and relaxation period

A preliminary study on aerosol properties in the low and high troposphere

Contributors:

Doina Nicolae(1), Lucia Mona(2), Aldo Amodeo(2), Giuseppe D'Amico(2), Volker Freudenthaler(3), Christophe Pietras(4), Holger Baars(5), Michael Sicard(6), Iwona S. Stachlewska(7), Eleni Marinou(8), Anna Gialitaki(8), Maria Tsichla(8), Eleni Drakaki(8), Ioanna Tsikoudi(8), Livio Belegante(1), Camelia Talianu(1), Dragos Ene(1), Michail Mytilinaios(2), Sergio Ciamprone(2), Aldo Giunta(2), Nikolaos Papagiannopoulos(2), Moritz Haarig(5), Cristofer Jimenez(5), Ronny Engelmann(5), Dietrich Althausen(5), Karsten Hanbuch(5), Birgit Heese(5), Elizaveta Basharova(5), Rico Hengst(5), Ulla Wandinger(5), Adolfo Comeron(6), Constantino Muñoz-Porcar(6), Alejandro Rodríguez-Gómez(6), Alex Zenteno(6), Dominika Szczepanik(7), Dongxiang Wang(7), Rafał Fortuna(7), Vassilis Amiridis(8), Alexandra Tsekeri(8), Alexandros Papayannis(9), Maria Mylonaki(9), Christina Anna Papanikolaou(9), Aleksandros Pietruczuk(10), Arnoud Apituley(11), Patrick Freville(12), Daniele Bortoli(13,14), Maria João Costa(13,14), Lucas Alados-Arboledas(15)(16), J. L. Guerrero-Rascado(15)(16), J. A. Bravo-Aranda(15)(16), D. Bermejo-Pantaleón(15)(16), M. J. Granados-Muñoz(15)(16), P. Ortiz-Amezcua(15)(16), M. M. Jiménez-Martín(15)(16), Mika Komppula(17), Xiaoxia Shang(17), Maria Rita Perrone(18), Ferdinando de Tomasi(18), Salvatore Romano(18), Philippe Goloub(19), Thierry Podvin(19), Nicolas Pascal(19), Qiaoyun Hu(19), Diofantos Hadjimitsis(20)(21), Rodanthi-Elisavet Mamouri(20)(21), Argyro Nisantzi(20)(21), Ina Mattis(22), Davide Dionisi(23), Gian Luigi Liberti(23), Dimitrios Balis(24), Kalliopi Artemis Voudouri(24), Michailidis Konstantinos(24), Zoran Mijic(25), Maja Kuzmanoski(25), Luka Ilic(25)

(1) *National Institute of R&D for Optoelectronics, Magurele, Romania*
(2) *Consiglio Nazionale delle Ricerche - Istituto di Metodologie per l'Analisi Ambientale (CNR-IMAA), Potenza, Italy*
(3) *Meteorological Institute, Ludwig-Maximilians University, Munich, Germany*
(4) *Centre National de la Recherche Scientifique - Institut Pierre Simon Laplace, Paris, France*
(5) *Leibniz Institute for Tropospheric Research, Leipzig, Germany*
(6) *CommSensLab, Dept. of Signal Theory and Communications, Universitat Politècnica de Catalunya (UPC), 08034, Barcelona, Spain*
(7) *University of Warsaw, Faculty of Physics, Warsaw, Poland*
(8) *National Observatory of Athens ISAARS, Athens, Greece*
(9) *National Technical University of Athens, Physics Department*
(10) *Institute of Geophysics, Polish Academy of Sciences, Warsaw*
(11) *KNMI - Royal Netherlands Meteorological Institute, The Netherlands*
(12) *Observatoire de Physique du Globle (OPGC-LaMP), France*
(13) *Institute for Earth Sciences, Evora, Portugal*
(14) *Physics Department, Evora University, Evora, Portugal*
(15) *Andalusian Institute for Earth System Research (IISTA-CEAMA), Granada, Spain*
(16) *Applied Physics Department, University of Granada, Granada, Spain*
(17) *Finnish Meteorological Institute (FMI), Kuopio, Finland*
(18) *University of Salento, Physics Department, Lecce, Italy*
(19) *Lille 1 University - Science and Technology, Lille, France*
(20) *Cyprus University of Technology, Dep. of Civil Engineering and Geomatics, Limassol, Cyprus*
(21) *ERATOSTHENES Centre of Excellence, Limassol, Cyprus*
(22) *DWD Meteorological Observatory Hohenpeissenberg, Germany*
(23) *Consiglio Nazionale delle Ricerche - Istituto di Scienze Marine (CNR-ISMAR), Rome, Italy*
(24) *Laboratory of Atmospheric Physics, Physics Department, Aristotle University of Thessaloniki, Thessaloniki, Greece*
(25) *IPB – Institute of Physics Belgrade, Serbia*

Contents

About EARLINET/ACTRIS

The European Aerosol Research Lidar Network, EARLINET, was established in 2000 as a research project with the goal of creating a quantitative, comprehensive, and statistically significant database for the horizontal, vertical, and temporal distribution of aerosols on a continental scale [Pappalardo et al., 2014]. Since then EARLINET has continued to provide the most extensive collection of ground-based data for the aerosol vertical distribution over Europe.

EARLINET is part of ACTRIS (Aerosols, Clouds and Trace gases Research Infrastructure). ACTRIS is a pan-European initiative consolidating actions amongst European partners producing high-quality observations of aerosols, clouds and trace gases. ACTRIS was accepted into ESFRI Roadmap in 2016 and is now in the implementation phase.

Methodology

This analysis is organized as part of the ACTRIS initiative for studying the changes in the atmosphere during the COVID-19 lockdown. With their high temporal and vertical resolution, lidars give comprehensive information on the atmospheric structure, its dynamics, and its optical properties.

The scope of the analysis is twofold: a) to monitor the atmosphere's structure during the lockdown and early relaxation period in Europe; b) to identify possible changes due to decreased emissions, by comparison to the aerosol climatology in Europe.

The study is organized in two parts:

1. **The analysis of January-April 2020 period**, based on measurements performed and processed at the individual stations, following pre-existent operation procedures. Measurements are collected on EARLINET schedule (three times per week:
    - Monday around local noon;
    - Monday after local sunset;
    - Thursday after local sunset).

   Data are processed in a decentralized way by each station, using their own algorithms or the Single Calculus Chain (SCC), and submitted to the EARLINET/ACTRIS database. Quality Control procedures are applied automatically on the data during the submission of the data to the EARLINET/ACTRIS database (https://www.earlinet.org/index.php?id=293). These procedures assure the technical quality of each data file. Additional controls on optical properties identify the data of highest quality (level 2 data). Level 1 data should be carefully handled by the data users, taking into account the critical issue identified by the quality control procedures. Both Level 1 and Level 2 data are available at https://www.earlinet.org/index.php?id=125). Only Level 2 data are currently directly available on ACTRIS data portal (http://actris.nilu.no/).

2. **An intensive observation campaign in May 2020**, following specific procedures. Measurements are collected on the campaign schedule (each day, two times per day: A) around noon; B) after sunset). Data are processed in a centralized way by the SCC, with specific configurations and settings, and made publically available through a THREDDS server in near-real time (NRT).

The near-real time campaign in May 2020

Introduction

During this campaign, the NRT capability of the EARLINET-ACTRIS was to be facilitated and demonstrated. Therefore, the lidars measured in an intensified schedule, at least twice per day (minimum two hours at noon, and minimum two hours after sunset). For data evaluation the SCC was used. The SCC is a tool for the automatic analysis of aerosol lidar measurements developed within EARLINET network [D'Amico et al., 2015, D'Amico et al., 2016; Mattis et al., 2016]. The main aim of SCC is to provide a data processing chain that allows all EARLINET stations to retrieve, in a fully automatic way, the aerosol backscatter and extinction profiles, starting from the raw lidar data collected by the lidar systems they operate. All input parameters needed to perform the lidar analysis are stored in a database to keep track of all changes which may occur for any EARLINET lidar system over the time, assuring the traceability of the data.

The data products calculated by the Single Calculus Chain / individual algorithms depend on the configuration of the lidar system (i.e. the available channels):

- **b1064** – the aerosol backscatter coefficient at 1064nm, calculated from the elastic channel (1064nm) with the Fernald-Klett algorithm; assumption of the lidar ratio at 1064nm is required
- **b532** – the aerosol backscatter coefficient at 532nm, calculated from the elastic channel (532nm) with the Fernald-Klett algorithm; assumption of the lidar ratio at 532nm is required
- **b355** – the aerosol backscatter coefficient at 355nm, calculated from the elastic channel (355nm) with the Fernald-Klett algorithm; assumption of the lidar ratio at 355nm is required
- **d532** – the linear particle depolarization ratio at 532nm, calculated from the combination of polarization channels at 532nm
- **d355** – the linear particle depolarization ratio at 355nm, calculated from the combination of polarization channels at 355nm
- **e532** – the aerosol extinction coefficient at 532nm, calculated from the Raman signals at 607nm with the Raman algorithm

- **e355** – the aerosol extinction coefficient at 355nm, calculated from the Raman signals at 387nm with the Raman algorithm
- **b(e)532** – the aerosol backscatter coefficient at 532nm, calculated from the combination of elastic (532nm) and Raman (607nm) channels
- **b(e)355** – the aerosol backscatter coefficient at 355nm, calculated from the combination of elastic (355nm) and Raman (387nm) channels

Depending on the design of the lidar, Raman channels can be operated during daytime (if the lidar system is equipped with optics/detectors optimized for the reduction of the sky background), or only during nighttime. As such, the related data products in general differ from day to night, in terms of evaluation approach.

Out of all the retrieved data products, this study focuses on b532 and d532 only, as being commonly available from many stations, both during daytime and nighttime. However, further analysis will include also other optical products (aerosol extinction coefficients, Angstrom exponents, lidar ratios), as well as synergy products (fine and coarse mode volume concentrations).

The aerosol backscatter coefficient is a measure of the aerosol load. The linear particle depolarization is a measure of the aerosol non-sphericity. These physical quantities were averaged within two different altitude ranges to investigate the aerosol variability related to the boundary layer and the free troposphere. The low troposphere is here defined up to 3 km altitude, where local influences are still possible. The high troposphere is defined from 3 km up to 7 km, where typically long-range transport of aerosols occurs and local influences are no longer present. Moreover, the average over the daytime and the nighttime is provided separately per each altitude range.

The average values are provided at 532 nm, as this is a wavelength at which the majority of the lidars operate. This wavelength is also preferable for a first analysis because many available satellites, models and passive sensors provide information in the visible range. For those sites for which only backscatter at 355 nm was available, the values were scaled to 532 nm considering a backscatter Angstrom exponent of 1. No wavelength dependence has been regarded for the particle depolarization ratio.

The number of profiles used for calculation of the mean values is reported in white, for the others no full information necessary for calculations of the mean values was available. Being an intensive parameter, the linear particle depolarization ratio values are considered significant only when the aerosol load is high enough to allow the depolarization characterization. Specifically, the values that are satisfying simultaneously the following three criteria, are used for the averaging procedures: backscatter > 5×10^{-7} $m^{-1}sr^{-1}$ and error_backscatter/abs(backscatter) < 50% and error_depolarization/abs(depolarization) < 50%. The average values are reported only for those parameters that were measured at least 3 times within the considered slot of measurement (e.g. daytime low troposphere).

This first analysis is based on the data processed by the SCC and directly public on the THREDDS server in NRT. These datasets are not fully quality control because the 2 quality control steps (manual checks at station level and automatic centralized quality control procedure at data center level) currently running on the EARLINET "standard" datasets are here not applied for the aim of a NRT data provision.

After the closure of the campaign, a re-analysis will be done for improving atmospheric molecular profiles used into the inversion, additionally all participating stations are called to a carefully inspection of all the profiles for screening the SCC outputs and selecting data suitable for the upload on the EARLINET/ACTRIS database. These selected datasets will be then uploaded on the EARLINET/ACTRIS database and screened automatically through the EARLINET/ACTRIS quality control procedures. All these steps will produce a quality control improved datasets for this campaign publically available on the EARLINET/ACTRIS database fully traceable and version controlled (expected by June 30th). Once the re-analyzed data are made public on the EARLINET/ACTRIS database, NRT data will be removed from the THREDDS server and stored centrally at the EARLINET/ACTRIS local database and available on request for specific study.

For the purposes of the campaign, the measurements were submitted and processed in the near-real time in maximum 12h after the end of the mandatory noon and nighttime observation. Each station performed some visual inspection for selecting the most suitable profile for the fast analysis of aerosol, situation and highlighting the presence of clouds not correctly captured by the SCC Cloud masking module. However, this is still preliminary data until the full set of the quality assurance / quality control (QA/QC) procedures is applied and the re-analysis is performed and finalized.

Participating lidar stations

EARLINET currently comprises 31 active stations. Out of these, 21 participated in this campaign, covering different regions over Europe. These stations operate either automatic and/or remotely controlled instruments, or they are located in regions where a complete lock-down was/is not effective.

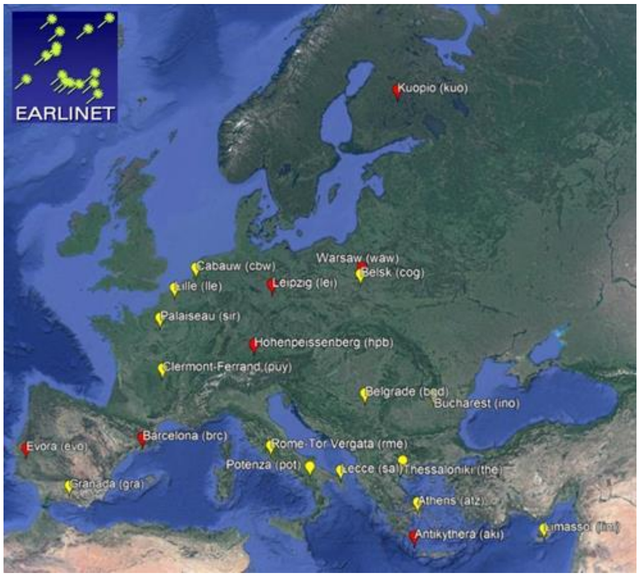

Lidar stations providing measurements of the aerosol profiles daily: a) in yellow, stations measuring 2 times per day; b) in red, stations providing quasi-continuous observations. In general, no measurements are performed during precipitation and presence of low clouds.

Location	**Coordinates**
Athens	37.9600 N, 23.7800 E, 212 m
Barcelona	41.3930 N, 2.1200 E, 115 m
Belsk	51.8300 N, 20.7800 E, 180 m
Bucharest	44.3480 N, 26.0290 E, 93 m
Cabauw	51.9700 N, 4.9300 E, 0 m
Clermont-Ferrand	45.7610 N, 3.1110 E, 420 m
Evora	38.5678 N, -7.9115 E, 293 m
Granada	37.1640 N, -3.6050 E, 680 m
Kuopio	62.7333 N, 27.5500 E, 190 m
Lecce	40.3330 N, 18.1000 E, 30 m
Leipzig	51.3527 N, 12.4339 E, 125 m
Lille	50.6117 N, 3.1417 E, 60 m
Limassol	34.6700 N, 33.0400 E, 10 m
Hohenpeissenberg	47.8019 N, 11.0119 E, 974 m
Palaiseau	48.7130 N, 2.2080 E, 156 m
Potenza	40.6000 N, 15.7200 E, 760 m
Roma-Tor Vergata	41.8330 N, 12.6500 E, 110 m
Thessaloniki	40.6300 N, 22.9500 E, 50 m
Warsaw	52.2100 N, 20.9800 E, 112 m
Antikythera	35.8600 N, 23.3100 E, 193 m
Belgrade	44.8557 N, 20.3913 E, 89 m

Specific data products

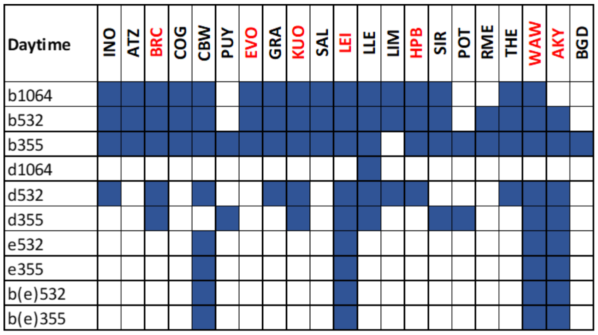

Daytime	INO	ATZ	BRC	COG	CBW	PUY	EVO	GRA	KUO	SAL	LEI	LLE	LIM	HPB	SIR	POT	RME	THE	WAW	AKY	BGD
b1064	■	■	■	■	■		■	■	■	■	■	■	■	■	■			■	■		
b532	■	■	■	■	■		■	■	■	■	■	■	■	■	■		■	■	■	■	
b355	■	■	■	■	■	■	■	■	■	■	■	■		■	■	■	■	■	■	■	■
d1064												■									
d532	■		■		■			■	■		■	■	■	■				■	■	■	
d355			■			■			■		■	■			■	■			■	■	
e532					■						■								■	■	
e355					■						■								■	■	
b(e)532					■						■								■	■	
b(e)355					■						■								■	■	

Data products calculated for each station during daytime; in red, stations providing quasi-continuous measurements.

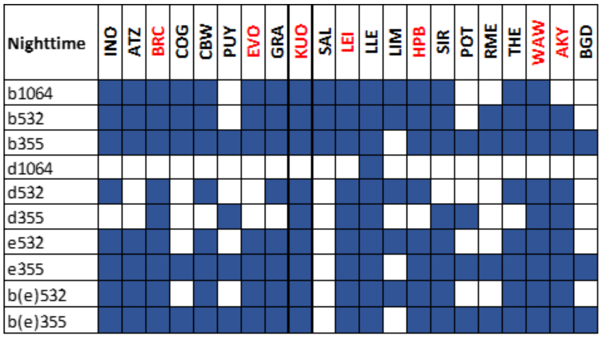

Nighttime	INO	ATZ	BRC	COG	CBW	PUY	EVO	GRA	KUO	SAL	LEI	LLE	LIM	HPB	SIR	POT	RME	THE	WAW	AKY	BGD
b1064	■	■	■	■	■		■	■	■	■	■	■	■	■	■			■	■		
b532	■	■	■	■	■		■	■	■	■	■	■	■	■	■		■	■	■	■	
b355	■	■	■	■	■	■	■	■	■	■	■	■		■	■	■	■	■	■	■	■
d1064												■									
d532	■		■		■			■	■		■	■	■	■				■	■	■	
d355			■			■			■		■	■			■	■			■	■	
e532	■	■	■		■		■	■	■		■	■	■	■	■			■	■	■	
e355	■	■	■	■	■	■	■	■	■		■	■		■	■	■	■	■	■	■	■
b(e)532	■	■	■		■		■	■	■		■	■	■	■	■			■	■	■	
b(e)355	■	■	■	■	■	■	■	■	■		■	■		■	■	■	■	■	■	■	■

Data products calculated for each station during nighttime; in red, stations providing quasi-continuous measurements.

Meteorological context

After the exceptionally dry and sunny April 2020, May 2020 was accompanied by many vicissitudes of weather. During the first days of the month, cold arctic air masses were present in North Europe, combined with the frontal occlusions over Scandinavia. Atmospheric circulation above Europe was described by zonal flow, with no large horizontal temperature or pressure gradients. Higher pressure field was observed around a 500hPa ridge above West Europe, while lower pressure fields around a trough, that occurred above East Europe, resulted in dry and settled weather. In the middle of the first week (1-7 May), a high pressure system from North-West England interacted with a low pressure system from southwest, delivering increasingly brisk easterly winds (50mph) in the English Channel. At the same time in Eastern Europe, a surface warm front, extending from Belarus across South-East Europe into the Eastern Mediterranean, was moving slowly, causing rain and local thunderstorms for several days. Moreover, a well-developed low-pressure system from the Atlantic advected towards North-East Europe, running into the block of high pressure in central areas, resulting in a well-shaped frontal occlusion through central and Eastern Europe.

During the second week (8-15 May), the circulation can be described by upper high-pressure fields above Balkans and deep trough/low over western Iberian Peninsula, along with cold arctic air-masses aloft over North Europe. A cold front was shaped on the South-Eastern side of the North Atlantic anticyclone (with surface pressure-center 1036hPa), blocking these colder air-masses from the Arctic. The sharp frontal system, extending from North-West Russia across North-East Europe into the Alpine region, moved across central Europe with a relatively slow speed and storms along the leading frontal boundary. Thick, high and cold ice clouds formed, mainly above France, Germany and Poland (11 May). As a result, much colder weather spread behind the front, but very warm temperatures remained in front of it. Temperatures of several degrees Celsius below zero were recorded over Western Europe (Zugspitze, Germany -7,7^{o}C). In combination to these conditions, snowfall occurred in several regions along the front, especially over Poland and Belarus. Similar atmospheric circulation was observed at the end of the second week (12-13 May), with the large cold pool remaining over Northern and Eastern Europe, gradually vanishing on the few following days. Ahead of the frontal line, a warm air-mass in the Eastern Mediterranean affected the region, causing completely different weather conditions.

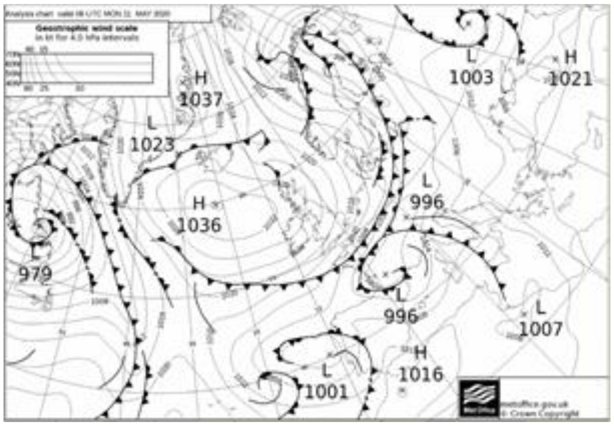

Surface Analysis for 11 May 2020 06UTC (source: Met Office; Aktuelle Wetterkarten http://www1.wetter3.de/)

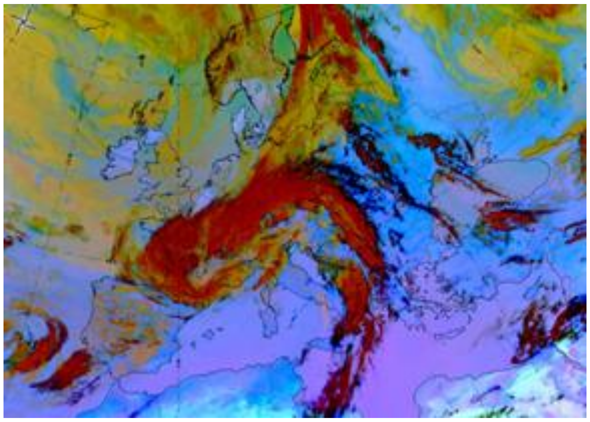

SEVIRI Dust RGB Satellite Image for 11 May 2020 12 UTC (source: http://eumetrain.org/ePort_MapViewer/)

During the third week (14-21 May), the large-scale dynamics provoked a heat-wave, very rare for mid-May, which expanded across the southern Mediterranean from North Africa, spread into south Italy, southern Balkans, and Turkey. In addition, the 0^{o}C isotherm line was spreading across central Europe and separating the area into two different temperature fields. The atmospheric conditions were characterized by a well-developed low pressure system, spinning anti-clockwise above Azores and a high pressure system spinning clockwise over North Africa, and thus, causing a quite strong wind field, associated with the surface circulation. This resulted locally in severe south winds (50 knots) enriching central and East Mediterranean with dust loads from Africa. Record-breaking temperatures, apropos the season, were observed on Sunday 17th May, when the heat intensified further, leading peaks over 40°C (Antalya-Bolge, Turkey in 43.0 °C). The extremely warm air-mass remained over the area until mid-week and then slowly vanished, as the upper-level ridge over the Mediterranean collapsed. After this historically record-breaking heat-wave, a quite strong and large cold pool pushed from the North, began spreading across the East-South-East Europe into the Balkans and the Black Sea region, bringing much colder weather and much lower temperatures than long-term average for late May. Frost was recorded over Poland, Ukraine and Belarus, while very large hail fell in Godetch, Bulgaria. There was also interaction with high and low pressure fields over western and Eastern Europe, respectively. A ridge on the Iberian peninsula and a trough on top of Balkans, were pushed eastwards, resulting in surface cyclogenesis on the Eastern fields of the trough (Italy, Greece) combined with cloud formation at the end of the third week (20-21 of May). At the same time, another large trough with a very deep core (520gpm at 500hPa level), combined with surface cyclogenesis (rapidly intensifying with peak near 965 hPa), was covering part of the North Atlantic and Western Europe, moving towards North-East. The system delivered severe winds (115 km/h was reported along Western Ireland, 166 km/h in the Scottish Highlands) along with flooding events from heavy rainfall.

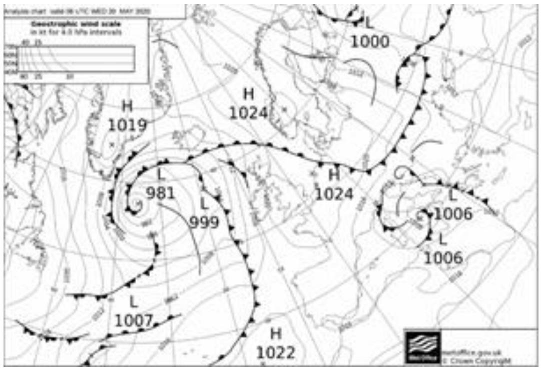

Surface Analysis for 20 May 2020 06UTC (source: Met Office; Aktuelle Wetterkarten http://www1.wetter3.de/)

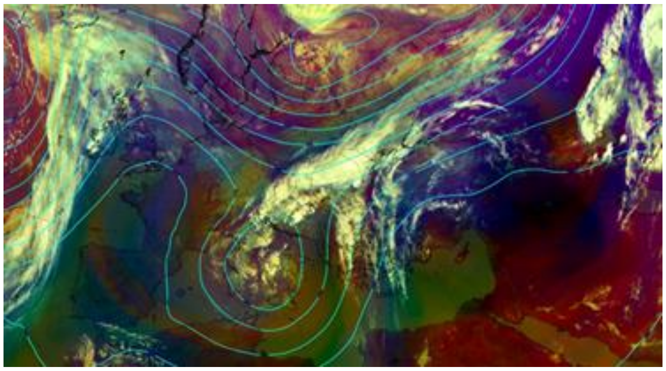

MSG Airmass RGB Satellite Image for 20 May 2020 09 UTC (source: http://eumetrain.org/ePort_MapViewer/)

During the last week (24-31 May), a frontal activity in combination with a classic dipole pattern was underway across European continent. A cold front over eastern and northern Europe at the beginning of the week, and another one over Northern Europe at the end, resulted in cloudy and rainy weather. An upper-level ridge has established over Western Europe, providing stability and warm temperatures, while a large upper low was located over Eastern Europe, with daily showers and thunderstorms. Weather remained cloudy and rainy across Eastern Europe and Mediterranean, with daily convective activity under the upper low. The frontal system brought additional rain over the Southern Balkan Peninsula, and especially over parts of Ukraine, South-Eastern Poland, South Belarus, and Western Russia. This pattern maintained over the east and South-East Europe until the end of the month.

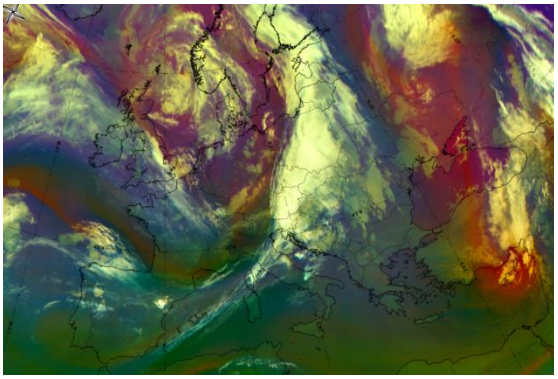

MSG Airmass RGB Satellite Image for 24 May 2020 00 UTC (source: http://eumetrain.org/ePort_MapViewer/)

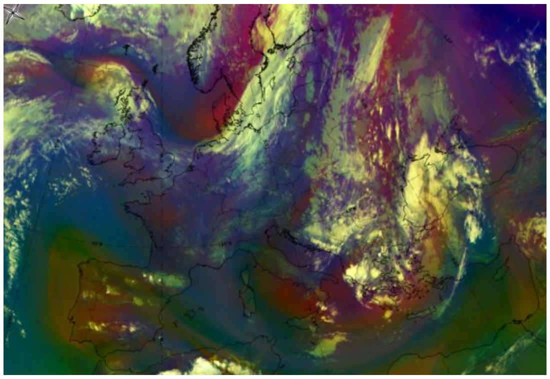

MSG Airmass RGB Satellite Image for 27 May 2020 18 UTC (source: http://eumetrain.org/ePort_MapViewer/)

Dust outbreaks

During the campaign period, the European region was affected with five dust outbreaks. More specifically, during 2-5 of May, a surface low pressure system over the Atlantic Ocean that was enhanced by a well-structured trough in the upper troposphere, resulted in the strong South winds that loaded dust mass above the Western Mediterranean. Dust mass was spread to the area of Portugal and, gradually, extended towards the East, thus affecting Spain. During 6-8 of May, the formation of a low pressure system over Egypt loaded dust mass from Morocco to the Western Mediterranean. At the same time, a deeper low pressure system above Morocco with high winds, gradually spread dust in parts of central and Eastern Europe and the Eastern Mediterranean until 13 of May. The most intense dust outbreak of the month was initiated on 12 of May, by a surface low pressure system over the dust sources of North Sahara, enhanced by a deep trough in the upper troposphere. This was associated with thick cloud cover. The low moved slowly to the Eastern Mediterranean, where it confronted a pool of cold air in the upper troposphere coming from North, enhancing the formation of a cyclonic system in the Adriatic Sea (on 20th of May). The cyclonic system led to precipitation and dust deposition in the Eastern Mediterranean and the Eastern Europe. Finally, during 26-28 of May a shallow low pressure system above Morocco, in combination with the anticyclonic circulation above the Eastern Mediterranean and central and Eastern Europe, led to a low intensity dust outbreak that affected the Western Mediterranean.

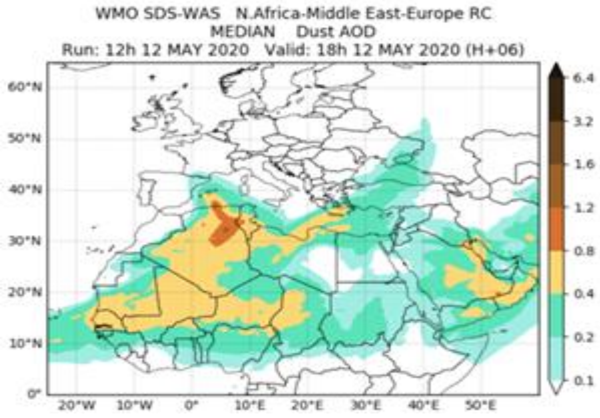

Ensemble Aerosol Optical Depth (source: WMO SDS-WAS: https://sds-was.aemet.es/forecast-products/dust-forecasts/ensemble-forecast)

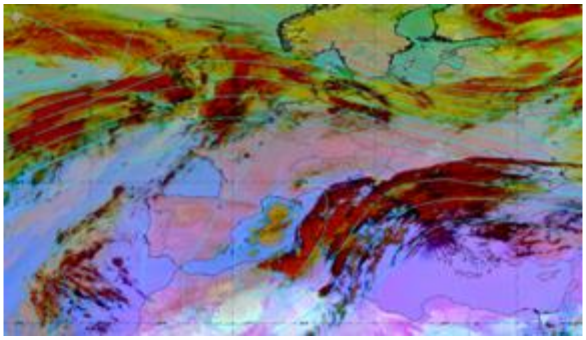

MSG-RGB Dust Satellite Image and Geopotential height at 500hPa for 18 May 2020 06UTC (source:http://eumetrain.org/ePort_MapViewer/)

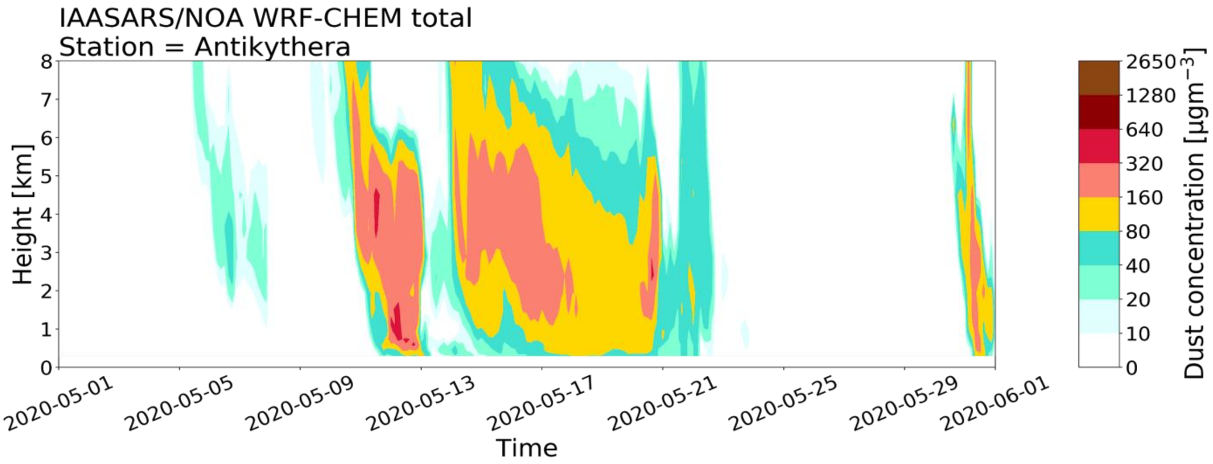

Hovmoller plot for WRF-Chem dust concentration in μgm^{-3} above the station of Antikythera, Greece.

Statistics of the measurements

All 21 stations performed measurements. In general, there were very few technical problems, except the Potenza station (from 16 May no observations due to laser failure). Many of the stations experienced days with unfavorable weather conditions for observations (rain or very low clouds saturating the lidar signal).

Out of the 1302 scheduled observations, 693 were performed, representing 53%. Although many stations have performed additional measurements, for the reason of ensuring equal sampling, only 2 datasets per day per station were selected for the analysis. The rest of the datasets are remaining available for detailed studies. In 27% of the cases, measurements could not be performed due to weather conditions (rain or very low clouds). Access to the laboratory and lack of personnel made the measurements impossible in 12% of the cases (especially in the first week), while only 8% of the measurements could not be performed due to technical problems, or instrument setting and check-ups.

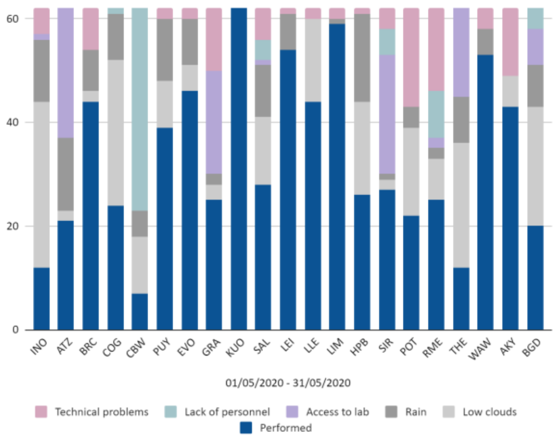

Measurement statistics

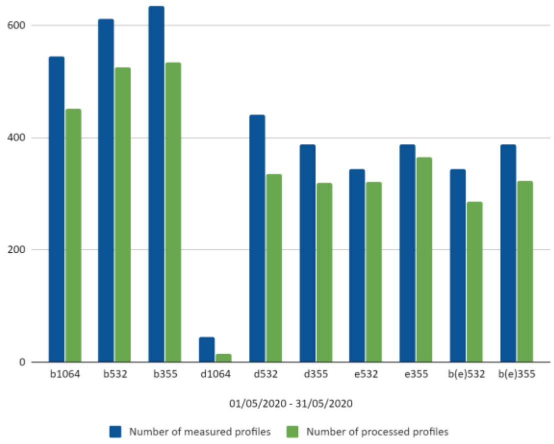

Data products statistics

From a total number of 4125 data products which could be calculated by the SCC from the performed measurements, 3473 were actually obtained and used in this analysis, representing 84%**.** This is a very good score for the SCC, considering that all pre-processing and processing algorithms are run in a completely automatic way. Most of the missing data products are due to the presence of low clouds in the measurements submitted for calculations. The clouds are screened out by the Cloud Masking module. In the case when after cloud screening the remaining data has no sufficiently high signal-to-noise-ratio, the optical products are not calculated.

Dynamics of the aerosol layers

Quicklooks below show the temporal variability of the aerosol layers in the vertical. Regions in the atmosphere with high content of aerosols or clouds are identified in red colors, while "clean" regions are shown in blue. For the stations with depolarization capabilities, the quicklook is shown for both the rangesquare corrected signal (aerosol load) and the volume depolarization ratio (aerosol anisotropy). Grey color indicates lack of measurement due to low clouds or precipitation.

The dynamic of the atmospheric structure, related to the space and time variation of the aerosol content, has been very diverse at the European scale during May 2020. Generally speaking, better conditions for the observation of aerosols, namely longer periods of clear skies, were met at all stations in the second half of the campaign.

During week 1 (1-7 May) low-level clouds were mostly present in central Europe (WAW, LEI, HPB). In the Iberian Peninsula, the campaign started with clear skies and a 2-day dust outbreak observed in EVO (1.5-4.5 km height, AOD_{532}~0.4) and later in BRC (up to 6 km height, AOD_{532}~0.4), and mid-level clouds settled. In the southeastern station of AKY the week was divided into three consecutive periods of clouds, clear sky and clouds.

During week 2 (8-14 May) very different conditions were observed all over Europe. KUO had cloud/rain conditions alternating with clear sky with virtually no aerosol. Low clouds and rain dominated in the western Mediterranean Basin. A polluted ABL was observed in AKY followed by the arrival of a Saharan dust outbreak on 10 May observed up to 5.5 km height and which reached the surface on 12 May. AOD_{532} peaked at ~0.5. A new dust outbreak hit the island on 13 May. Very diverse structure and conditions (clouds, rain, clear-sky) were observed in the continental stations of LEI and WAW.

Clear skies generally marked week 3 (15-21 May) in the south (EVO, BRC, AKY), while mostly cloudy conditions were present in the continental stations (LEI, HPB and WAW) with a clear-sky window in the middle of the week (17, 18 and 19 May) at LEI and HPB. AKY was under the influence of a dust outbreak started on week 2 until 19 May. A peak in AOD_{532} of ~0.8 was observed on 15 May. One day after its arrival the dust plume coupled to the ABL (see the quicklook of volume depolarization ratio for AKY). In KUO clouds dominated the scene.

Week 4 (22-29 May) is marked with generally clear skies above Europe: the whole week in southern Europe (EVO, BRC, AKY) and also in the north (KUO), and at the beginning and at the end of the week in the continental stations of LEI, HPB and WAW. In those 3 stations, the middle of the week was marked with clouds and some rain. In KUO pollen activity was detected on the quicklooks of volume depolarization ratio.

Kuopio (KUO)

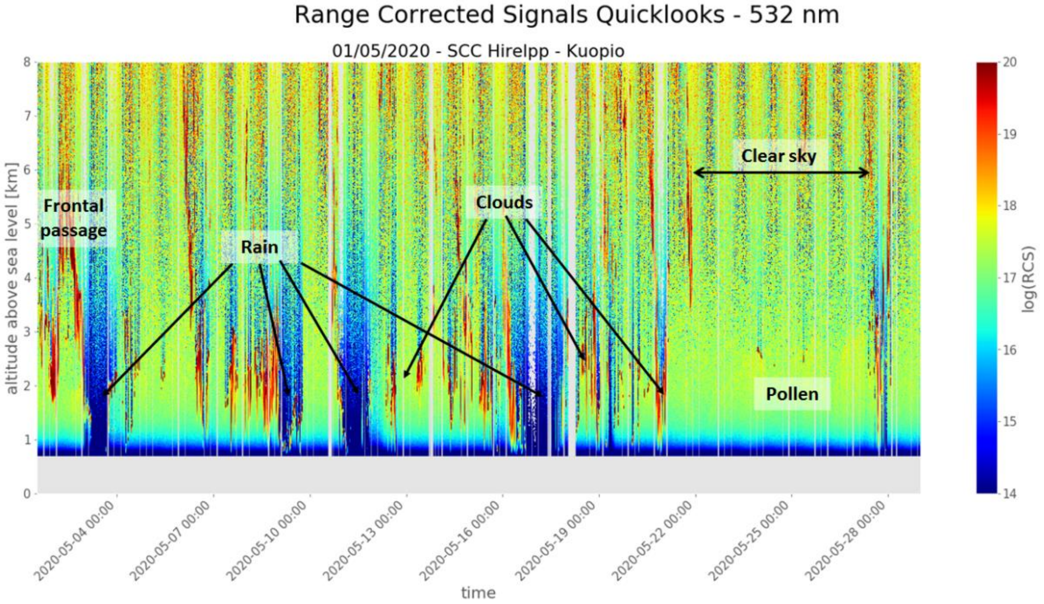
Range Corrected Signals Quicklooks - 532 nm
01/05/2020 - SCC Hirelpp - Kuopio
altitude above sea level [km]
0
1
2
3
4
5
6
7
8
Frontal passage
Rain
Clouds
Clear sky
Pollen
log(RCS)
14
15
16
17
18
19
20
2020-05-04 00:00
2020-05-07 00:00
2020-05-10 00:00
2020-05-13 00:00
2020-05-16 00:00
2020-05-19 00:00
2020-05-22 00:00
2020-05-25 00:00
2020-05-28 00:00
time

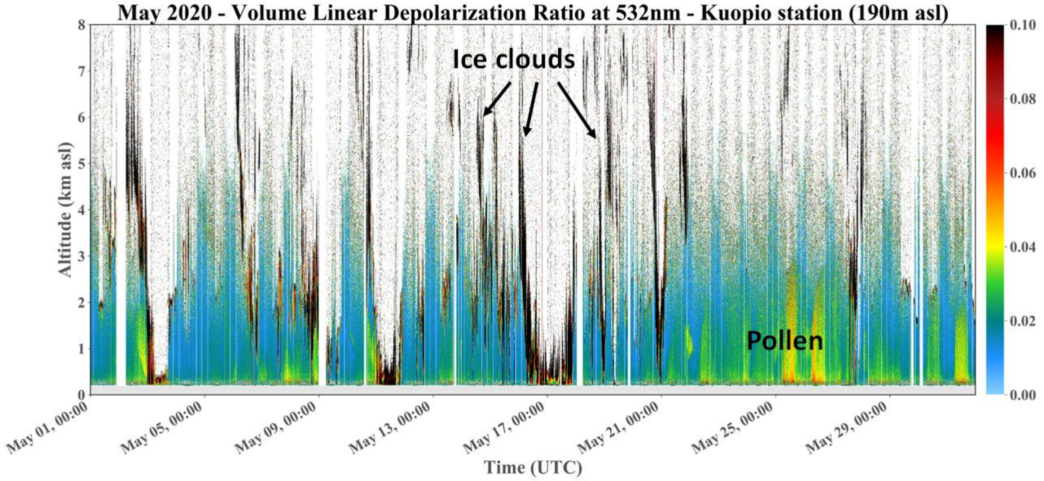
May 2020 - Volume Linear Depolarization Ratio at 532nm - Kuopio station (190m asl)
Altitude (km asl)
0
1
2
3
4
5
6
7
8
Ice clouds
Pollen
0.00
0.02
0.04
0.06
0.08
0.10
May 01, 00:00
May 05, 00:00
May 09, 00:00
May 13, 00:00
May 17, 00:00
May 21, 00:00
May 25, 00:00
May 29, 00:00
Time (UTC)

Leipzig (LEI)

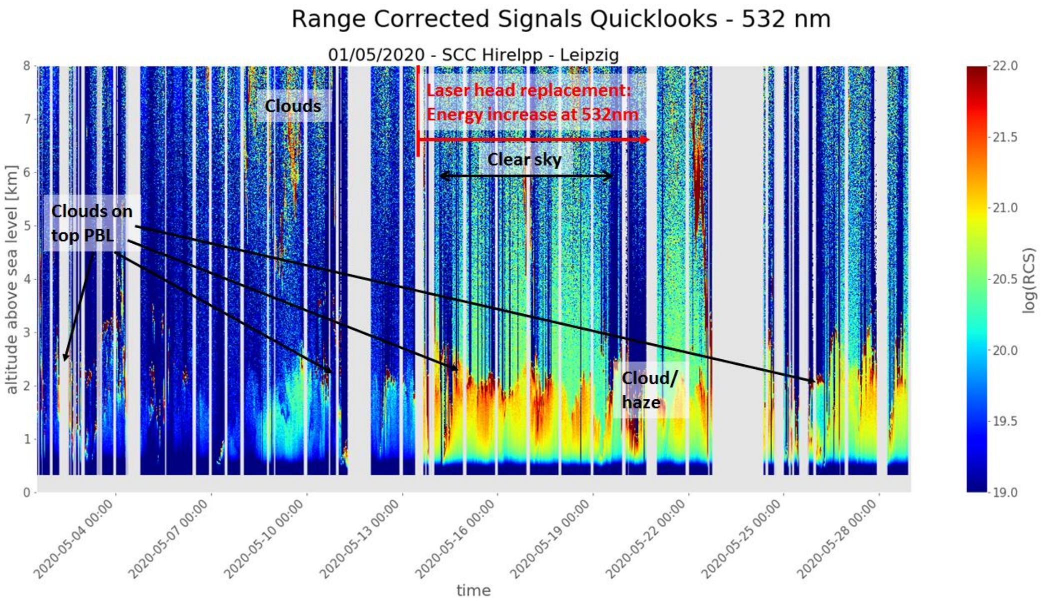
Range Corrected Signals Quicklooks - 532 nm
01/05/2020 - SCC Hirelpp - Leipzig
Clouds
Laser head replacement:
Energy increase at 532nm
Clear sky
Clouds on
top PBL
Cloud/
haze
altitude above sea level [km]
0
1
2
3
4
5
6
7
8
2020-05-04 00:00
2020-05-07 00:00
2020-05-10 00:00
2020-05-13 00:00
2020-05-16 00:00
2020-05-19 00:00
2020-05-22 00:00
2020-05-25 00:00
2020-05-28 00:00
time
log(RCS)
19.0
19.5
20.0
20.5
21.0
21.5
22.0

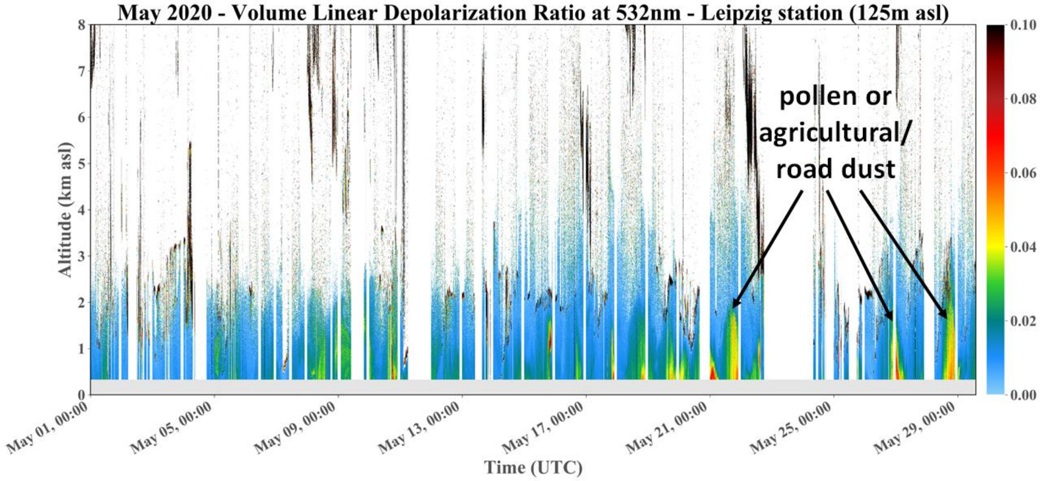
May 2020 - Volume Linear Depolarization Ratio at 532nm - Leipzig station (125m asl)
pollen or
agricultural/
road dust
Altitude (km asl)
0
1
2
3
4
5
6
7
8
May 01, 00:00
May 05, 00:00
May 09, 00:00
May 13, 00:00
May 17, 00:00
May 21, 00:00
May 25, 00:00
May 29, 00:00
Time (UTC)
0.00
0.02
0.04
0.06
0.08
0.10

Hohenpeissenberg (HPB)

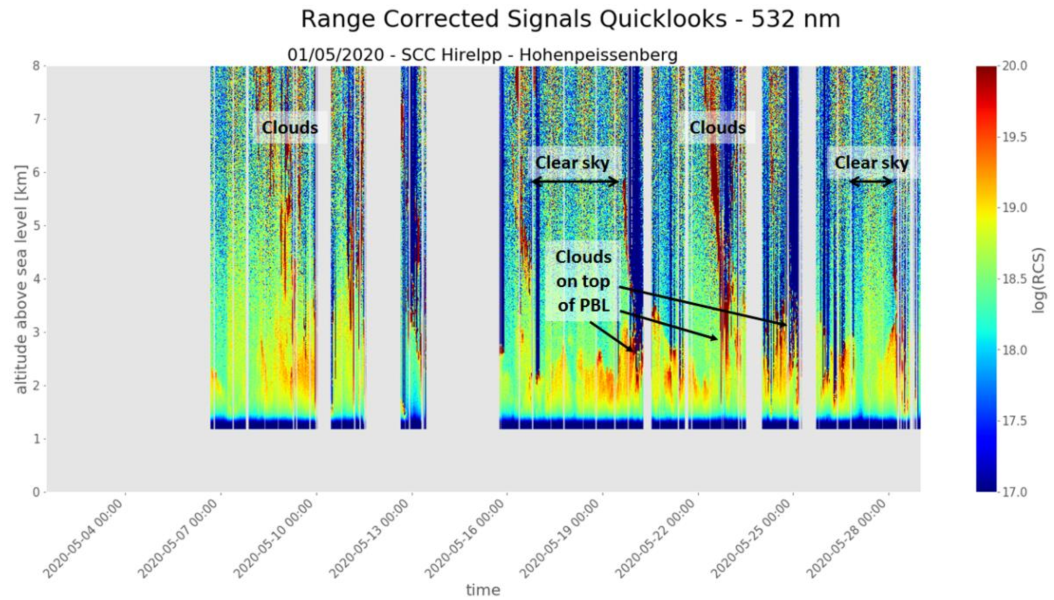

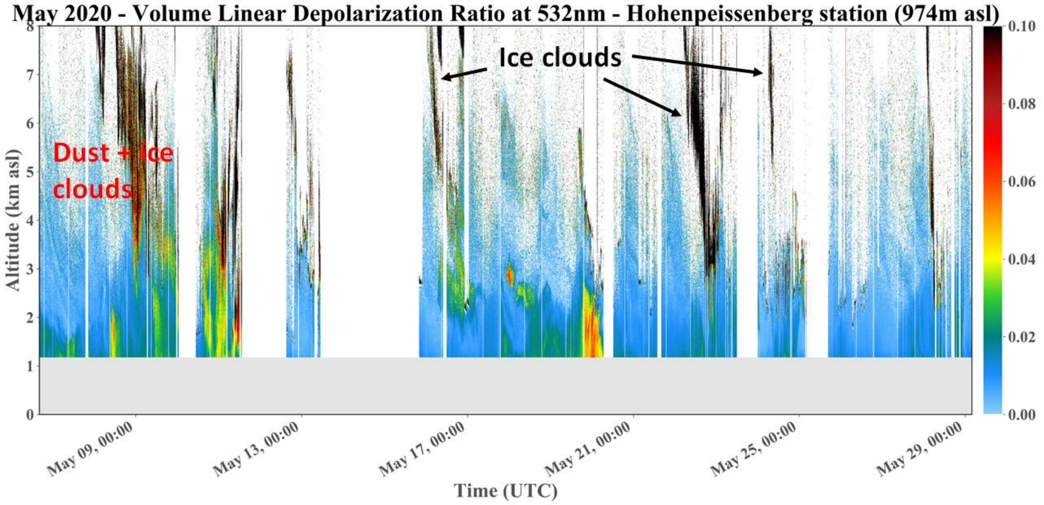

Warsaw (WAW)

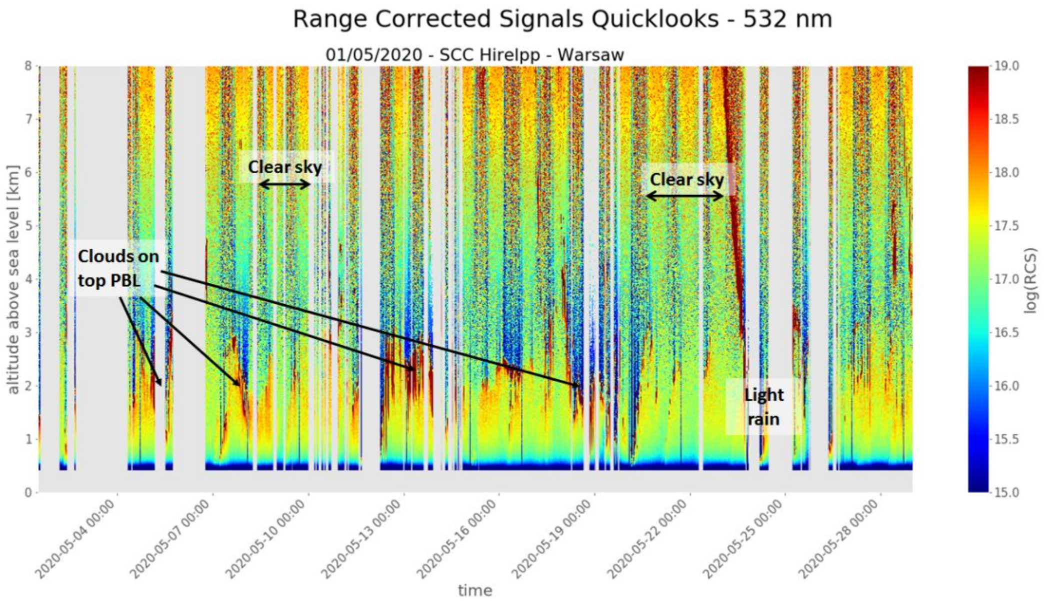
Range Corrected Signals Quicklooks - 532 nm
01/05/2020 - SCC Hirelpp - Warsaw
altitude above sea level [km]
0
1
2
3
4
5
6
7
8
Clear sky
Clear sky
Clouds on top PBL
Light rain
2020-05-04 00:00
2020-05-07 00:00
2020-05-10 00:00
2020-05-13 00:00
2020-05-16 00:00
2020-05-19 00:00
2020-05-22 00:00
2020-05-25 00:00
2020-05-28 00:00
time
log(RCS)
15.0
15.5
16.0
16.5
17.0
17.5
18.0
18.5
19.0

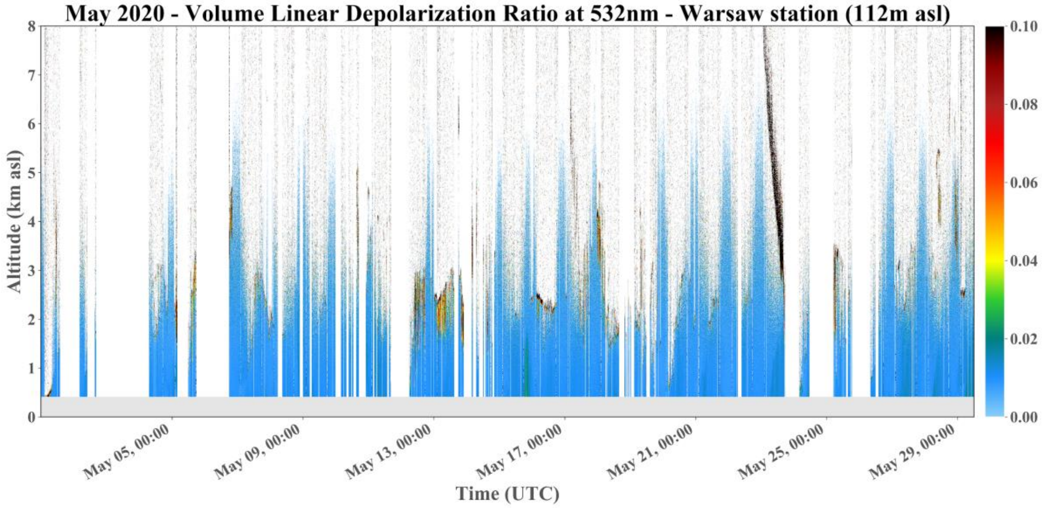
May 2020 - Volume Linear Depolarization Ratio at 532nm - Warsaw station (112m asl)
Altitude (km asl)
0
1
2
3
4
5
6
7
8
May 05, 00:00
May 09, 00:00
May 13, 00:00
May 17, 00:00
May 21, 00:00
May 25, 00:00
May 29, 00:00
Time (UTC)
0.00
0.02
0.04
0.06
0.08
0.10

Barcelona (BRC)

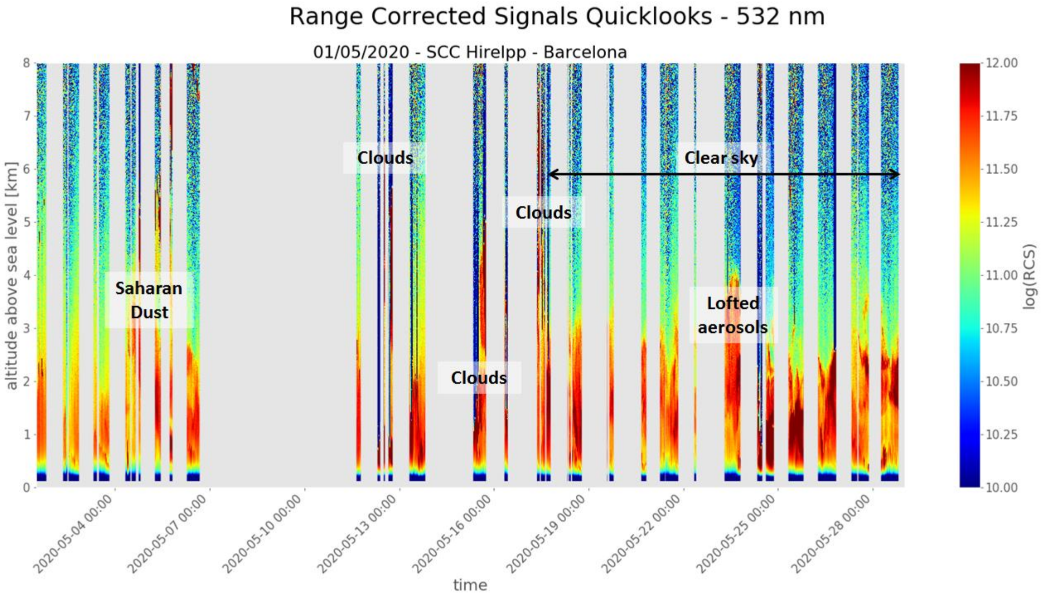

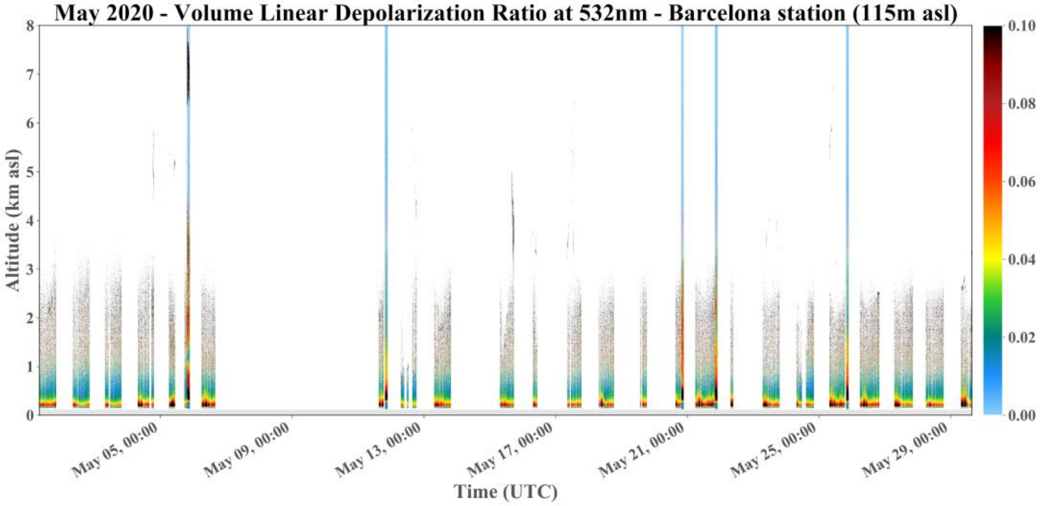

Evora (EVO)

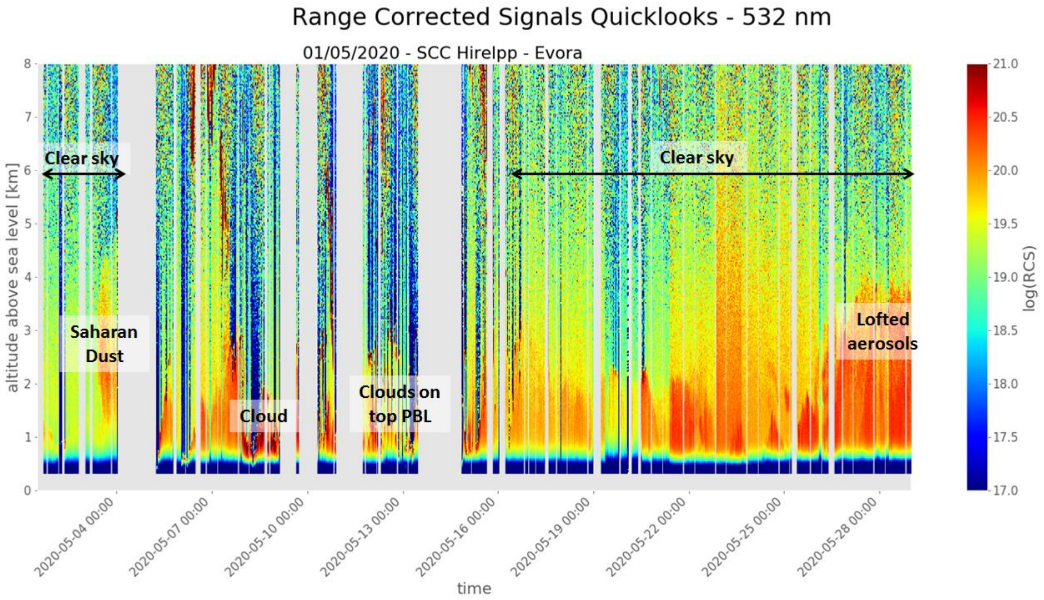
Range Corrected Signals Quicklooks - 532 nm
01/05/2020 - SCC Hirelpp - Evora
altitude above sea level [km]
0
1
2
3
4
5
6
7
8
time
2020-05-04 00:00
2020-05-07 00:00
2020-05-10 00:00
2020-05-13 00:00
2020-05-16 00:00
2020-05-19 00:00
2020-05-22 00:00
2020-05-25 00:00
2020-05-28 00:00
log(RCS)
17.0
17.5
18.0
18.5
19.0
19.5
20.0
20.5
21.0
Clear sky
Saharan Dust
Cloud
Clouds on top PBL
Clear sky
Lofted aerosols

Antikythera (AKY)

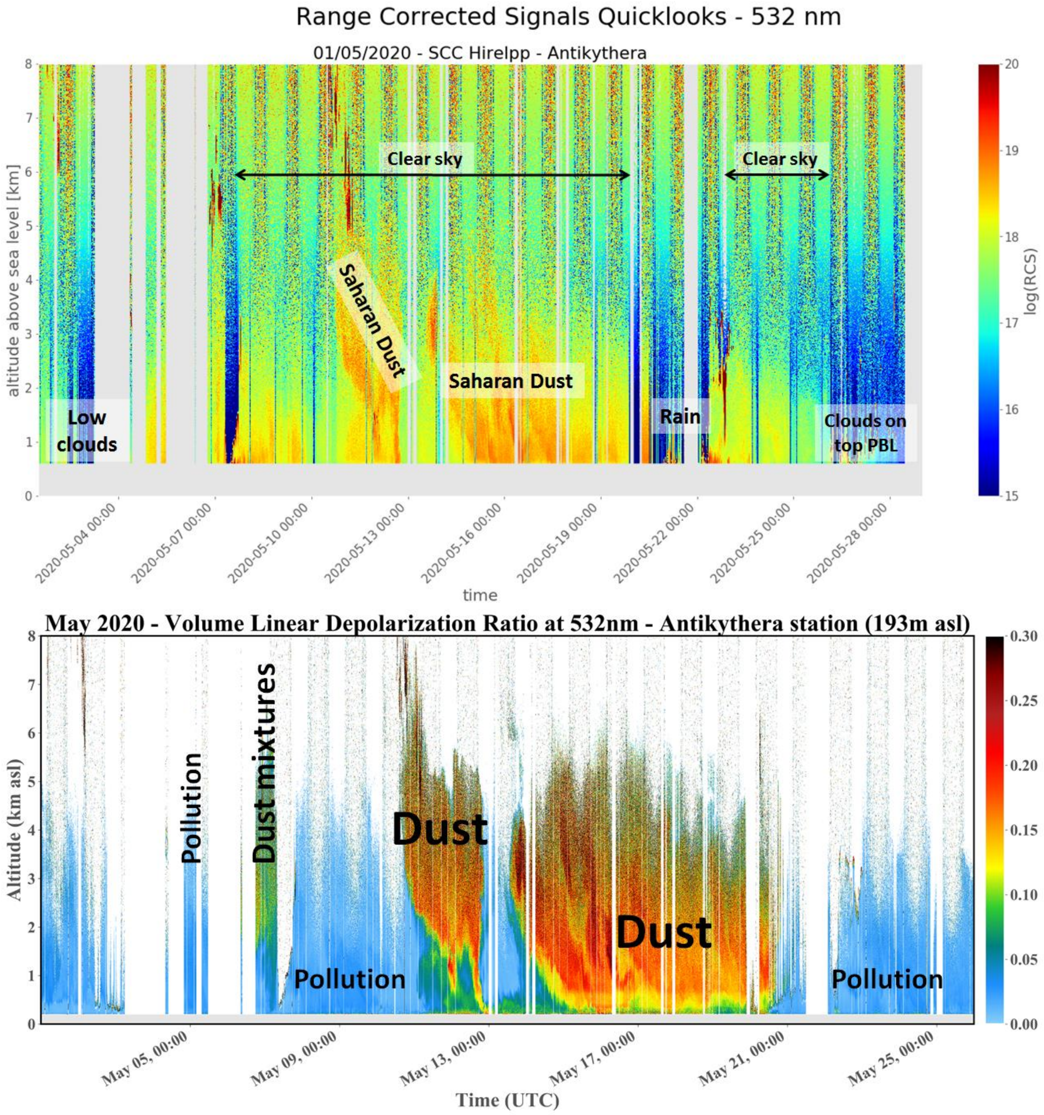

SIRTA (SIR)

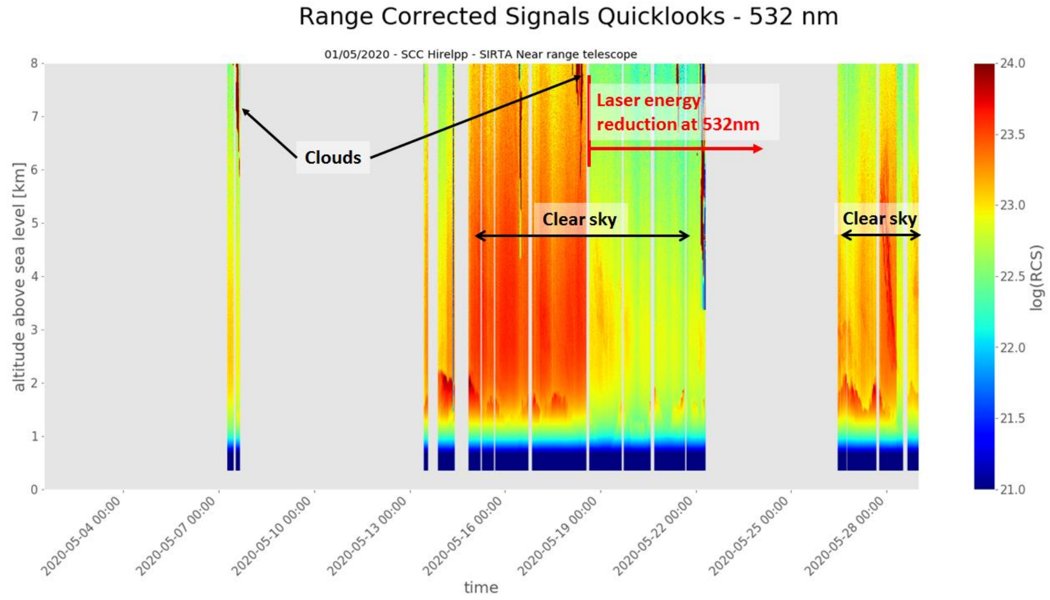

Mean values of the optical products in Europe

Next, we present a brief analysis for the entire time period of the NRT campaign (01-31 May 2020) of the average values for two optical parameters commonly measured at the observation sites: aerosol backscatter coefficient and particle linear depolarization ratio.

Aerosol backscatter coefficient is a measure of the aerosol load. Linear particle depolarization is a measure of the aerosol non-sphericity. Low troposphere is here defined up to 3 km altitude, where local influences are still possible. High troposphere is defined from 3 km up to 7 km, where typically long-range transport of aerosols occurs and no local influences are present. For sites for which only backscatter at 355 nm was available, the values were scaled to 532 nm considering a backscatter Angstrom exponent of 1. No wavelength dependence has been considered for the particle depolarization ratio. The number of profiles used for the mean calculation is reported in white.

Being an intensive parameter, the particle depolarization values are considered significant only when the aerosol load is high enough to allow the depolarization characterization. Specifically, the depolarization values satisfying the following criteria, satisfied simultaneously, are considered for the averaging procedures: backscatter > $5x10^{-7}$ $m^{-1}sr^{-1}$ and error_backscatter/abs(backscatter) < 50% and error_depolarization/abs(depolarization) < 50%.

Weekly means are reported only for parameters measured at least 3 times for the considered slot of measurement.

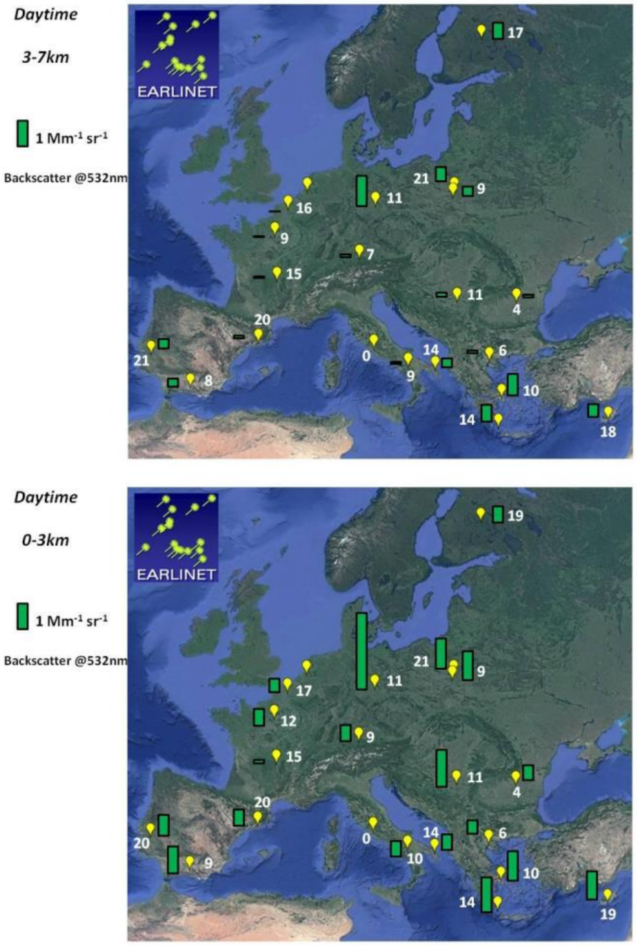

Monthly mean values of the aerosol backscatter coefficient (532 nm) for low troposphere (bottom panel) and high troposphere (upper panel) during daytime. The number of averaged profiles is reported in white.

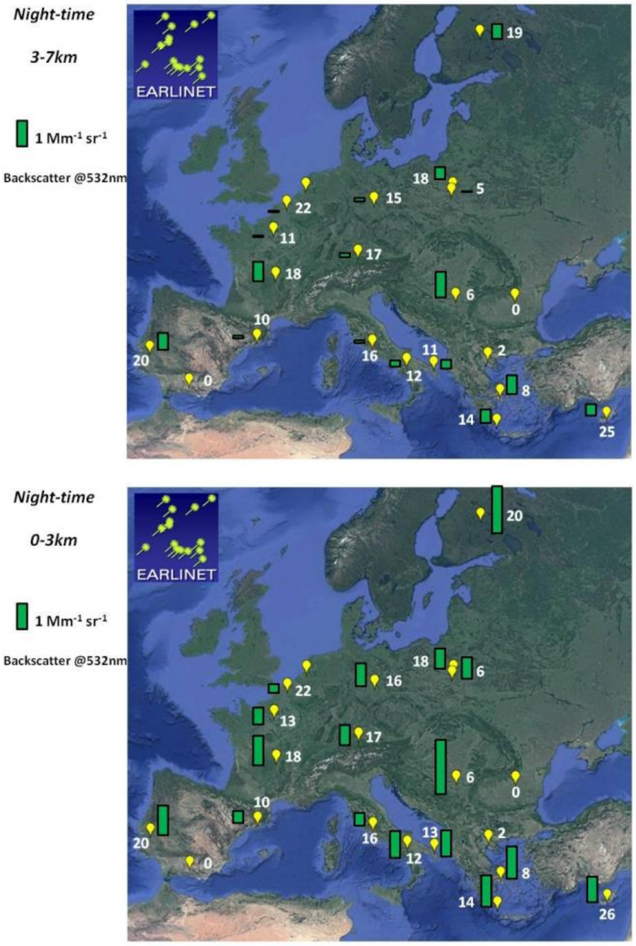

Monthly mean values of the aerosol backscatter coefficient (532 nm) for low troposphere (bottom panel) and high troposphere (upper panel) during nighttime. The number of averaged profiles is reported in white.

Aerosol backscatter at 532nm is typically higher in the Southern Europe respect to the Central and Northern Europe, because of the dust intrusion described in the meteorological context reported above. The almost equal mean values reported for daytime and nighttime observation both in the lowest troposphere and high troposphere is another signature of the relevance of the dust intrusion over Eastern Mediterranean stations (Italy, Greece, Cyprus). This is reflected also in the depolarization ratio values reported below, with values around 20% on average over the month both in low and free troposphere. Especially in Antikythera and in Limassol the depolarization ratio remains relatively constant during daytime and nighttime, within both tropospheric layers, in agreement with the vertical distribution and the time evolution of the dust plume transported over this region. On the contrary the big difference in daytime and nighttime backscatter mean value in the 0-3 km altitude range for Evora highlights the absence of dust and is the result of the marked PBL diurnal cycle.

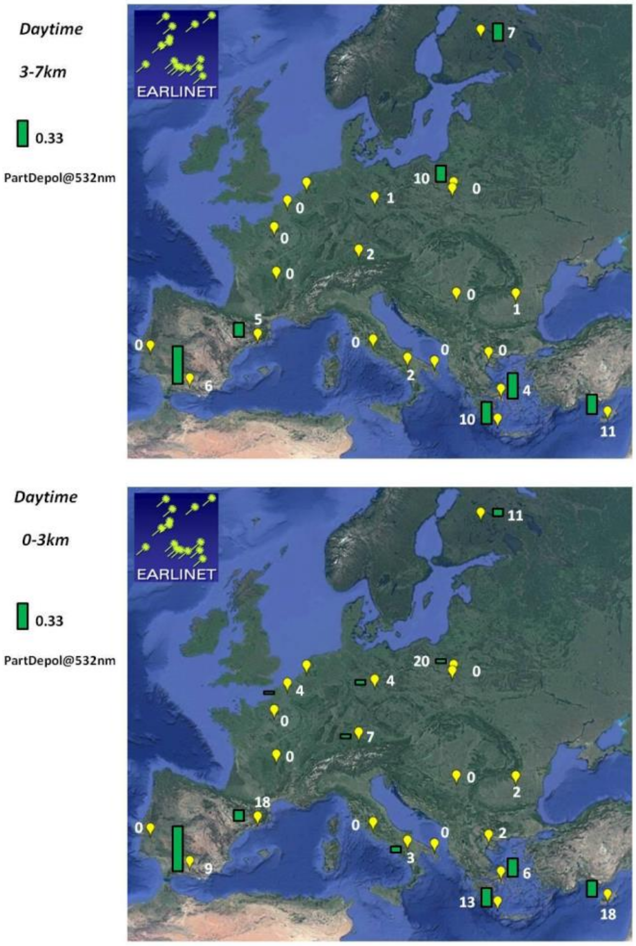

Monthly mean values of the particle linear depolarization ratio (532 nm) for low troposphere (bottom panel) and high troposphere (upper panel) during daytime. The number of averaged profiles is reported in white.

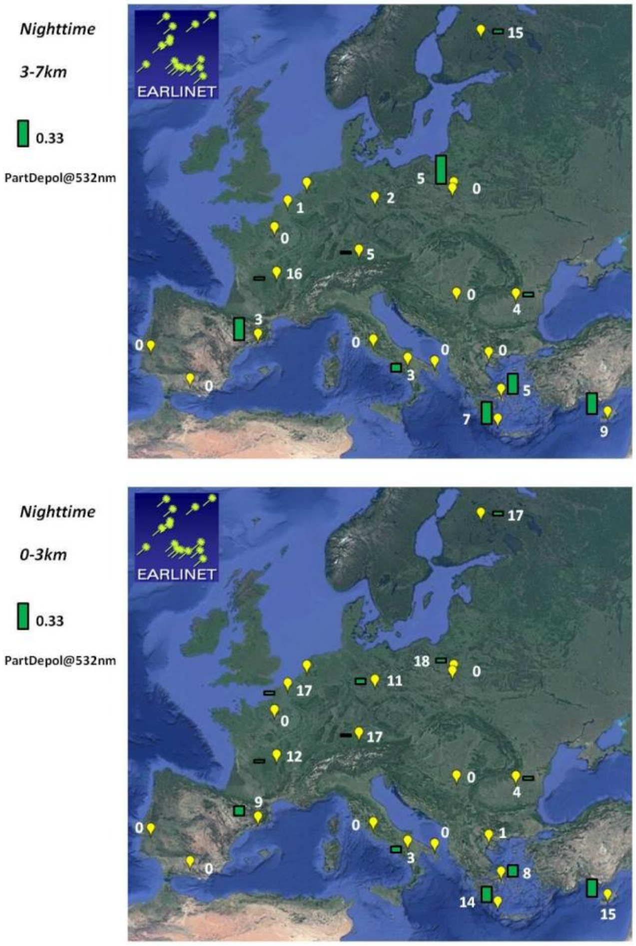

Monthly mean values of the particle linear depolarization ratio (532 nm) for low troposphere (bottom panel) and high troposphere (upper panel) during nighttime. The number of averaged profiles is reported in white.

Northern Europe instead is characterized by very low depolarization values and typically low values in the aerosol backscatter values both in low and high troposphere.

The analysis of January-May 2020 period

Introduction

In the previous section, preliminary results of the NRT data analysis of observations collected during the ACTRIS COVID-19 campaign are reported. This campaign was organized with a different sampling and data analysis and quality control procedures respect to the standard EARLINET ones. This was done for 1) fostering the collection of a larger dataset for the aim of the study and 2) providing NRT data. However this does not guarantee the quality of the data as currently available on the EARLINET/ACTRIS database.

EARLINET, established in 2000, changed over the years from a situation with a large variety of lidar system configurations and analysis algorithms to an harmonized, centralized, traceable and automatic data analysis in the ACTRIS operation phase (by 2025). Nowadays, in the middle of this evolution process, the observation collection, data analysis and data provision can be summarized as follows:

1) EARLINET stations perform measurements on the base of their resources (in terms of system capability and man power) but at least 3 times per week following the schedule established in 2000 (1 daytime on Monday and 2 nighttime on Monday and Thursday). Observations devoted to special event investigations and for Cal/Val missions are promoted. Continuous measurements are also available at some stations.

2) Data are provided not in NRT. The mandate for the EARLINET stations is to feed the EARLINET database submitting data every year: a station not providing data to the database for a full year is considered a gray station, entering a list of potentially not operating system. After 2 years of no submission of data the station is considered as not operational.

3) Data are processed at station level. Each station can use their own retrieval methods /algorithm or the common developed Single Calculus Chain. It is responsibility of the PI as representative person of the station to check the data and analysis result for spoiling eventual problems into the data outcomes which could also be the signature of instrument problems.

4) PI (or his/her authorized person) submit data to the EARLINET database. During this submission process, automatic quality control procedures perform technical checks on each individual file and reject files technically not compliant with EARLINET database. Further quality control procedures check data from the physical point of view: data compliant with these advanced quality controls are labeled as Level 2 data and are visible also on the ACTRIS data portal (https://actris.nilu.no/), while data not compliant with them are labeled as Level 1 data and should be treated by users with particular attention considering the reason of failure of these QC procedures. Level 1 data are currently available exclusively on the EARLINET database (https://www.earlinet.org/index.php?id=125).

Jan-May 2020 dataset

As reported above, there is no submission deadline within EARLINET. Because of the requirement of providing data at least once per year, PIs receive a notification when the station is not compliant. As such, the stations are providing data typically 1-1.5 year after the measurements have been performed.

In the frame of the ACTRIS initiative for investigating COVID-19 situation, a special effort was requested to the EARLINET stations to fully analyzed the data related to the observations of Jan-Apr 2020 period and make them available through the EARLINET database following the high quality standard. Ten stations provided data to the database by June 8th 2020 for the Jan-Apr 2020 period. Additionally Dushanbe has also provided some data. The rest of the stations did not provide data to the EARLINET database because of difficulties in working or analyzing the data due to COVID-19 restrictions, because no measurements were available during the period of COVID-19, and/or for upgrade of the systems (typical in this period of ACTRIS implementation). The 10 stations providing data for the Jan-Apr 2020 period are among the ones participating in the COVID-19 NRT campaign. This allows for a complete Jan-May analysis at these stations. Additionally the other 11 stations participating in the NRT campaign are added to the analysis enlarging the dataset.

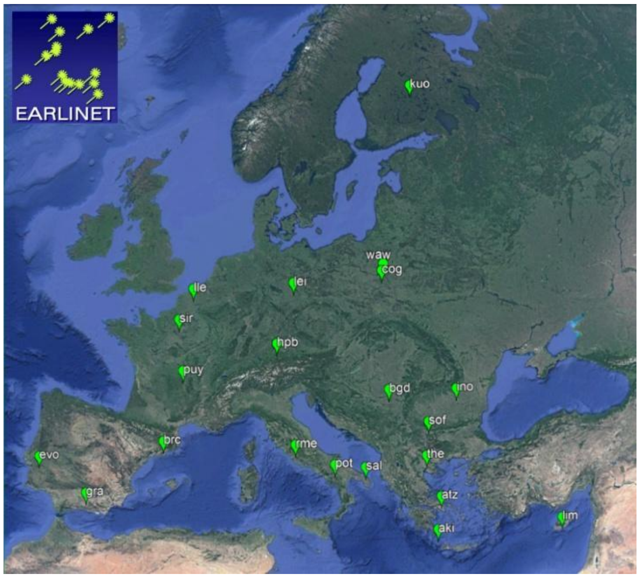

Lidar stations providing measurements of the aerosol profiles in Jan.-Apr. 2020

Location	**Coordinates**
Athens	37.9600 N, 23.7800 E, 212 m
Barcelona	41.3930 N, 2.1200 E, 115 m
Belsk	51.8300 N, 20.7800 E, 180 m
Bucharest	44.3480 N, 26.0290 E, 93 m
Clermont-Ferrand	45.7610 N, 3.1110 E, 420 m
Evora	38.5678 N, -7.9115 E, 293 m
Granada	37.1640 N, -3.6050 E, 680 m
Kuopio	62.7333 N, 27.5500 E, 190 m
Lecce	40.3330 N, 18.1000 E, 30 m
Leipzig	51.3527 N, 12.4339 E, 125 m
Lille	50.6117 N, 3.1417 E, 60 m
Limassol	34.6700 N, 33.0400 E, 10 m
Hohenpeissenberg	47.8019 N, 11.0119 E, 974 m
Palaiseau	48.7130 N, 2.2080 E, 156 m
Potenza	40.6000 N, 15.7200 E, 760 m
Roma-Tor Vergata	41.8330 N, 12.6500 E, 110 m
Sofia	42.6500 N, 23.3800 E, 550 m
Thessaloniki	40.6300 N, 22.9500 E, 50 m
Warsaw	52.2100 N, 20.9800 E, 112 m
Antikythera	35.8600 N, 23.3100 E, 193 m
Belgrade	44.8557 N, 20.3913 E, 89 m

The considered dataset for Jan-Apr period consists of 15137 files. Some Level 1 data are included for the study: Potenza and Thessaloniki data. For both stations the failed advanced QC procedure are related to absence of values for defined optical properties, so not affected the quality of reported values.

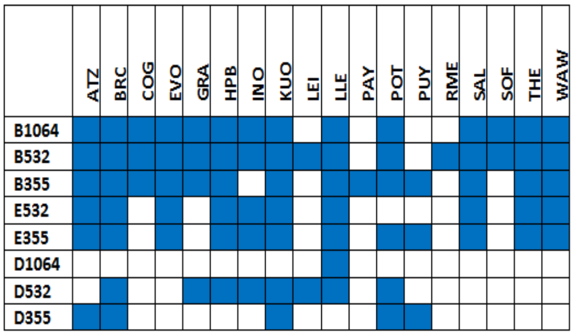

	ATZ	BRC	COG	EVO	GRA	HPB	INO	KUO	LEI	LLE	PAY	POT	PUY	RME	SAL	SOF	THE	WAW
B1064	■	■	■	■	■	■	■	■		■		■			■	■	■	■
B532	■	■	■	■	■	■	■	■	■	■		■		■	■	■	■	■
B355	■	■	■	■	■	■		■		■	■	■	■		■		■	■
E532	■	■		■		■	■	■		■					■		■	■
E355	■	■		■		■	■	■		■		■	■		■		■	■
D1064										■								
D532		■			■	■	■	■	■	■		■						
D355	■	■						■				■	■					

Data products calculated for each station during Jan-Apr 2020 period (updated on 8 June 2020)

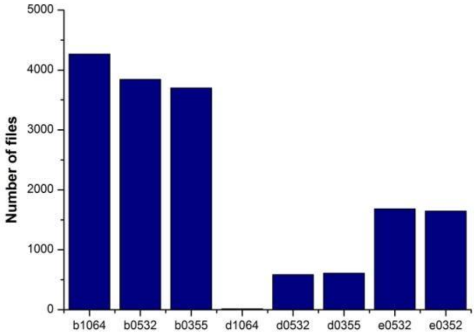

Data products statistics for Jan-Apr 2020 period (updated on 8 June 2020)

Meteorological context

JANUARY 2020

After the most devastating fire seasons in Australia, January 2020 was the warmest January on record, as the Polar Vortex (stronger than normal) trapped cold Arctic air in the polar circle. An unusual extreme warmth developing over Scandinavia, has led into record-breaking temperatures. (+19^{o}C Sunndalsøra-Norway: highest temperature ever measured in Scandinavia in winter months). In general, north Atlantic was developing explosive storms and intense cyclones almost on a daily basis. At 13th of January, the **extra-tropical cyclone "Brendan"** (central pressure 940hPa), rapidly intensified (bombogenesis) and moved towards Iceland and Western Europe, bringing severe winter storm. Finally the cyclone made landfall over the far western tip of Reykjanes peninsula. Another characteristic is that the evolving weather pattern is related to the positive North Atlantic Oscillation (NAO), favoring a stable ridging pattern over north Atlantic and Western Europe and a trapped low over Western Mediterranean for several days (Rex blocking). The trapped deep upper low (**cyclone Gloria** 17-25 January), lead to an extreme amount of rainfall over Spain and the Western Mediterranean, combined with major storm surge and destructive flooding.

FEBRUARY 2020

During February 2020, Europe was affected by large frontal systems (mostly cold fronts) moving from North Atlantic towards Europe and cold outbreaks. Moreover some significant cyclones were formed during February 2020, along with common winter frontogenesis. **Storm Dennis** (920hPa, 11-18 February) affected Western Europe less than a week after **Storm Ciara** (943hPa, 7-16 February), becoming one of the most intense extratropical cyclones ever recorded.

MARCH 2020

March is the beginning of meteorological spring, but first half of the month continued the winter pattern. Parts of Scandinavia were in the deep freeze and covered in thick snow across Lapland and higher Norway (Verlegenhuken-Norway -35.8°C, Enontekio Nakkala-Filand -30.7°C, Naumakka-Sweden -32.4°C). The second half of March, NAO turns into a negative phase. A powerful Rex block pattern developed with a significant Arctic cold outbreak from northern Russia into Europe and Mediterranean. In response to a deepening upper low, a surface low over the Eastern Mediterranean (central pressure 995 mbar, near Malta) resulted in excessive rainfall and flooding events, but also lots of snow over the Balkan Peninsula.

APRIL 2020

After an unusually intense arctic outbreak across Europe through the end of March, a powerful winter storm into Scandinavia and extremely cold mornings were present through the first days of April (-18°C Zugspitze-Germany, -16.8°C Kredarica-Slovenia April 1st). Spring finally arrived the second week of April, with a relatively fast return of warm (20-25°C) and stable weather across the European continent. A strong blocking high resulted in stable and dry conditions, with very high early April temperatures (23-27°C) across central Europe and Western Mediterranean (27.1°C Paris-Montsouris-France). Nevertheless, spring is the transitional period between winter and summer, thus fast weather changes take place. A quite impressive cold frontal passage (April 14th) across the East-central Europe, modified the situation from springtime weather into snowfall. Consequently, a few very cold mornings were verified in parts of central Europe (Lomnicky-Stit-Slovakia -16.3°C April 15th). After several days with cold weather, warmth returned to western and central Europe with some regions reporting temperatures above the 25°C threshold (Loznica-Serbia 29.3°C April 19th). The last week of April, an extensive upper ridge across the northern parts of Europe and a progressive dynamic pattern across Mediterranean brought excessive rainfall. Moreover, the ongoing progressive pattern against the extensive and powerful upper ridge, resulted also in advection of Saharan dust load from North Africa into Mediterranean and central Europe.

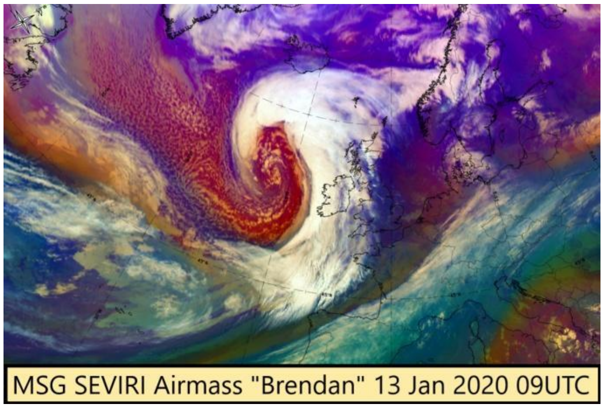

*MSG Airmass RGB Satellite Image for 13 January 2020 09UTC – “**Brendan**” (source: http://eumetrain.org/ePort_MapViewer/)*

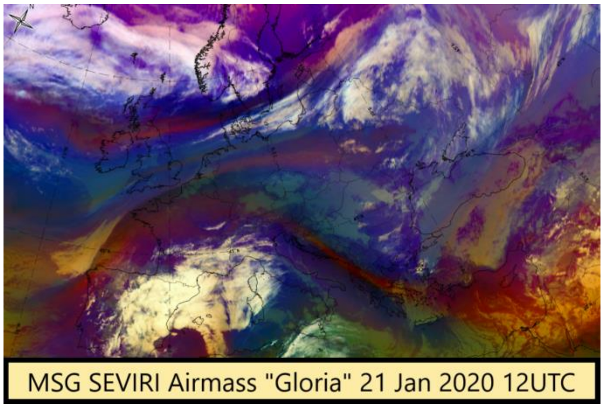

*MSG Airmass RGB Satellite Image for 21 January 2020 12UTC – “**Gloria**” (source: http://eumetrain.org/ePort_MapViewer/)*

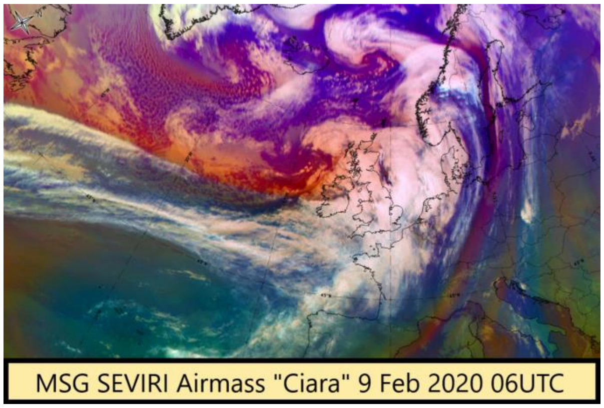

*MSG Airmass RGB Satellite Image for 9 February 2020 06UTC – “**Ciara**” (source: http://eumetrain.org/ePort_MapViewer/)*

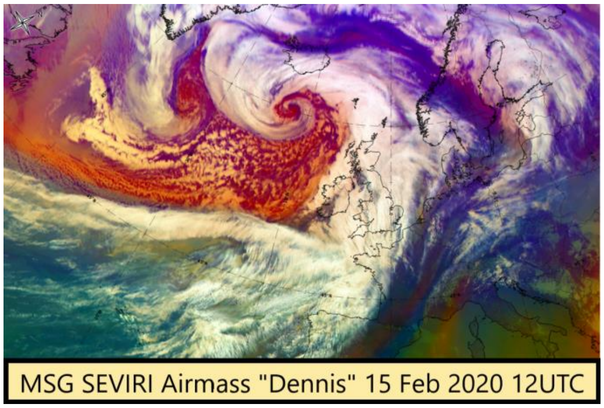

*MSG Airmass RGB Satellite Image for 15 February 2020 12UTC – “**Dennis**” (source: http://eumetrain.org/ePort_MapViewer/)*

Comparison of the January - May 2020 period with climatological values

Optical products at European scale

The first release of level 3 EARLINET climatological dataset is used as a reference for investigating potential deviation of the atmospheric aerosol content in the COVID-19 lockdown and relaxation period. The first Level climatological dataset (available at https://www.earlinet.org/index.php?id=125) is based on the highest quality control level data (Level 2) for the 2000-2015 period published on the WDCC-CERA database (https://doi.org/10.1594/WDCC/EARLINET_All_2000-2015).

The graphs below show the percentage difference with respect to the climatological value of the aerosol backscatter coefficient in the low and the high troposphere during the period January - May, calculated as the difference between Jan-May 2020 and the climatological normal monthly mean values for the 2000 – 2015 period: e.g. for each station the aerosol backscatter values collected in March 2020 are compared to the average of all the value collected at that station in all March occurring from 2000-2015.

Based on the availability of the climatological values, the following stations are considered in this analysis: Athens, Barcelona, Belsk, Bucharest, Evora, Granada, Lecce, Leipzig, Palaiseau, Potenza, Sofia Warsaw.

The positive values indicate a higher aerosol load than the climatological mean, while the negative a lower one. The analysis reports differences for the low troposphere (below 3 km asl) and free troposphere (between 3 and 7 km asl).

In the low troposphere a mean difference of +47% is observed in Jan-May period with a median value of +4%, showing on average a slightly increased aerosol load in the low troposphere. This is related to the high positive values (>100%) of the differences observed in the aerosol backscatter which could be related to specific situations.

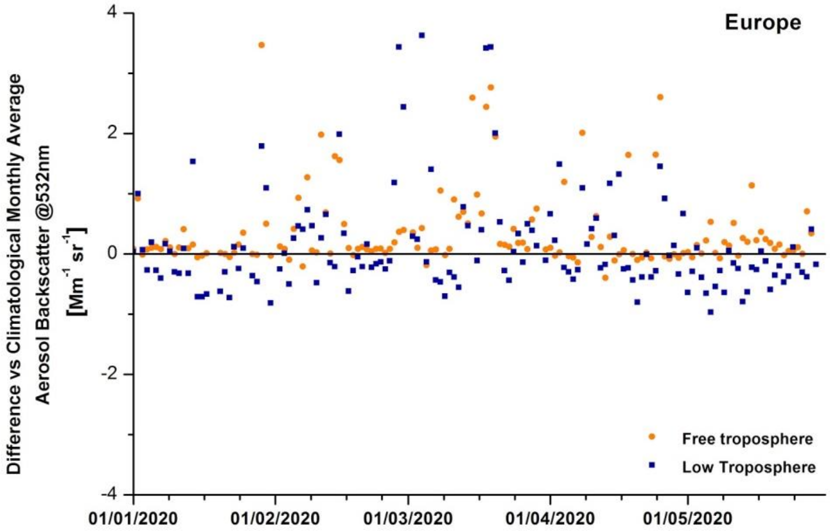

Time evolution of the aerosol backscatter coefficient (532 nm) in the low and high troposphere, as difference to the climatological values; average for all stations for Jan.-May 2020

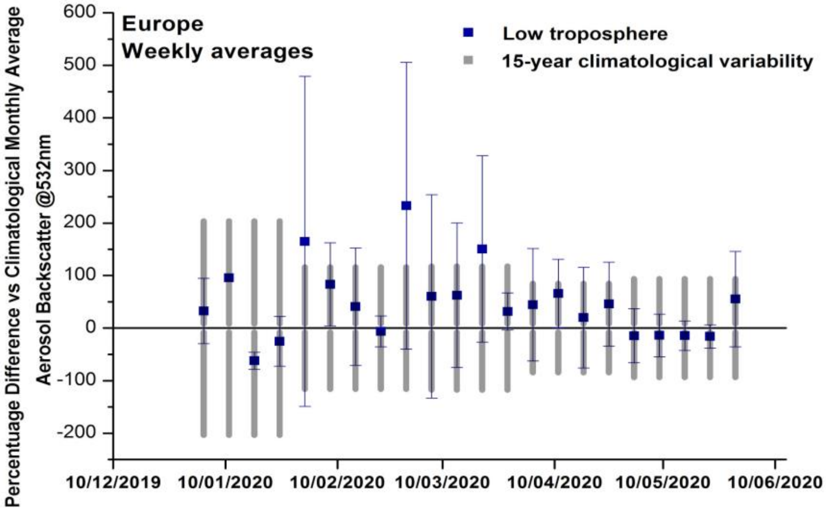

Percentage difference vs climatological values for the aerosol backscatter coefficient (532 nm) in the low troposphere; weekly average for all stations for Jan.-May 2020. Blue error bars report the weekly variability observed in 2020, gray vertical bars show the 15-year monthly variability over Europe

In the free troposphere, the values are in general higher than climatological means. In the scale of the whole continent, no specific behavior is observed when comparing the period before the COVID-19 lockdown (March 2020) and later on.

Optical products at regional scale

To better analyze the behavior of aerosol content in the low troposphere over European continent, the investigation is done at geographical cluster level. Five clusters are identified: Western Mediterranean, eastern Mediterranean, Central Europe, Eastern Europe and Northern Europe as reported in the following figure.

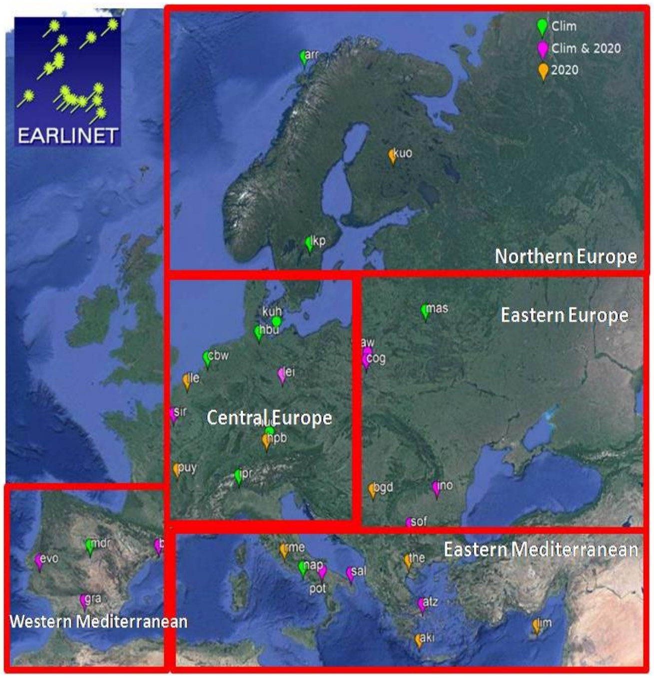

Identified geographical regions and EARLINET stations: stations reported in magenta have climatological dataset available and also data for 2020, stations reported in green provided climatological values used for cluster investigation and finally orange symbol represents stations for which climatological analysis is not available but provided data for 2020 analysis.

For each cluster, climatological monthly averages (black squares in the cluster plot analysis below) are calculated as average of the normal monthly average of the stations falling into the specific cluster. The standard deviation among the station averages provides an information on the spatial variability (reported as cyan error bar in the cluster plot analysis) and the mean of the monthly average standard deviation (red error bar in the plot below) provides instead an information about the temporal (and vertical) variability of the aerosol backscatter coefficient in the cluster in the 2000-2015 period.

The climatological values are compared versus the mean over the cluster of the station 2020 monthly averages (white diamonds).

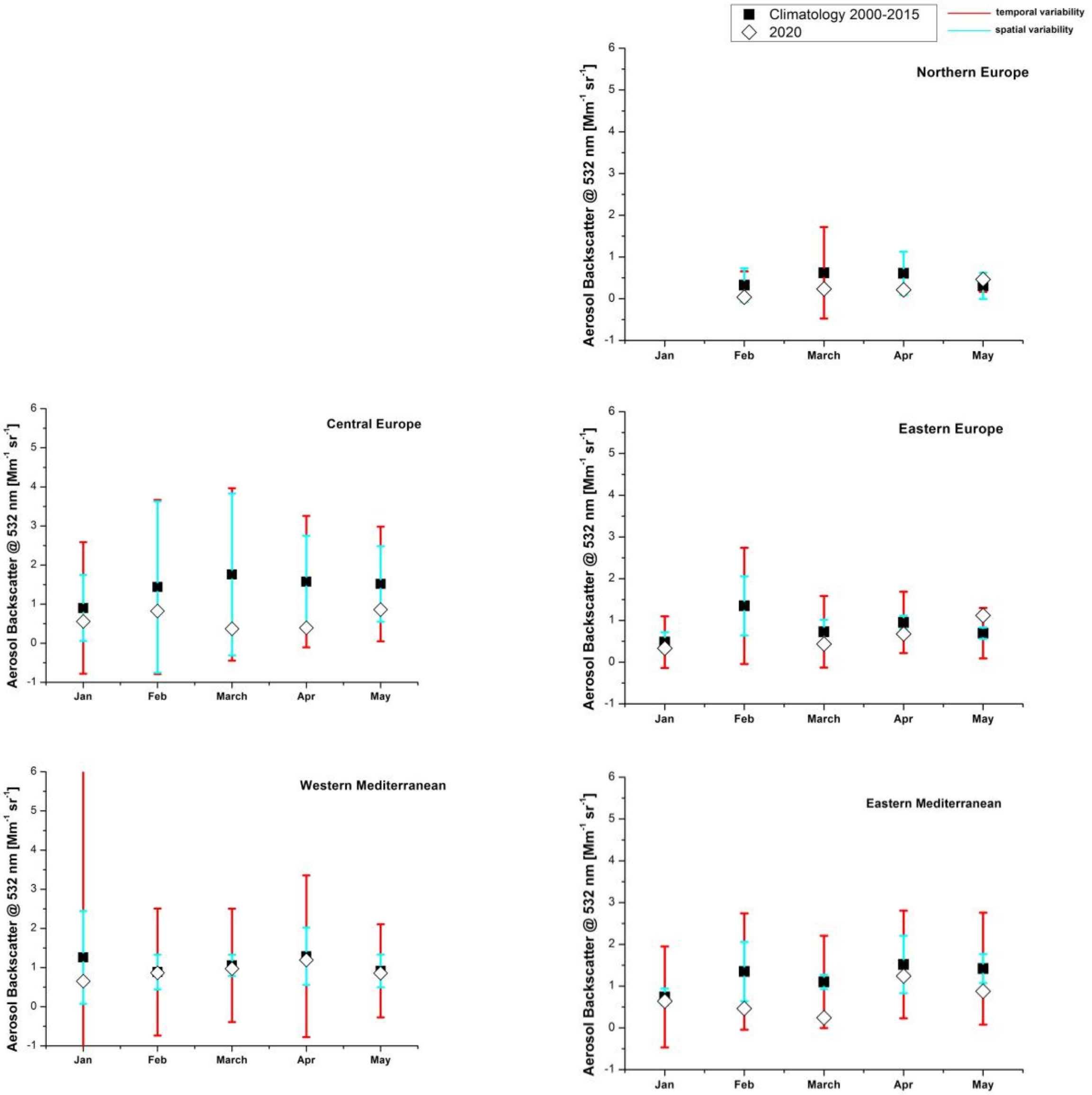

Geographical Cluster monthly averages of the aerosol backscatter coefficient (532 nm) in the low troposphere compared to corresponding climatological 2000.2015 monthly mean values (black squares). Mean temporal variability during the 2000-2015 period is reported as red error bars and the spatial variability within the cluster of the normal monthly average is reported as cyan error bar

When differentiating such analysis into five identified geographical clusters, it can be seen that in each one of the clusters a small tendency towards smaller values respect to the climatological ones seems to be present, but also that it is within the large variability observed in the 2000-2015 dataset. The differences observed in Central Europe and Eastern Mediterranean regions are more significant in the statistical sense: large deviations towards smaller values are observed for the low troposphere aerosol content in March, April and partially May (Central Europe) and in February and March (Eastern Mediterranean). The lower aerosol load already visible in February could be related to the lockdown in China resulting in less flights landing in these geo-regions of Europe. This is less visible for the Western Mediterranean as the dust occurrence in this area is so common that it disturbs the picture, although differences in the lower troposphere are also mainly negative. In Northern Europe and Eastern Europe, the effect in the lower troposphere is not as marked as in the rest of the regions, likely because there are less flights to China, so lockdown should not have so much effect as in the rest of Europe. However this aspect is to be better investigated.

In particular it has to be considered that EM and CE clusters are the most consolidated ones: more stations are located in those regions and they account for the longer climatological records (historical EARLINET stations). The WM cluster even if based on very long single station record is less populated and most of the data reported for Jan-Apr period is related to Evora observations which is a relatively new EARLINET station (so underrepresented in the climatological dataset). This first analysis points out the need for consolidated long term datasets in the different geographical regions and calls for more of stations in particular in Eastern and Northern Europe.

Further investigations are needed for better understanding the observed features. In particular an analysis will be done in terms of optical property profiles, aerosol layers and intensive properties which are related to the aerosol types.

Preliminary conclusions and further work

The preliminary analysis made on aerosol lidar data for the period January-May 2020 shows that by simply comparing the observed values with the climatological values from 2000-2015 is not sufficient to extract a clear conclusion on how much the COVID-19 lock-down has impacted the aerosols in the atmosphere. The changing meteorological conditions, the persistent periods with very low clouds and rain which made the lidar measurements difficult (therefore decreasing the number of measurements), as well as the presence of dust transported from North Africa to the Southern stations have reduced the statistical relevance.

Although it is clear from the analysis that the lock-down did not affected the high troposphere, for the low troposphere a certain effect can be seen, however within the climatological variability. Interestingly, when looking at the continental scale, decreased values of the aerosol backscatter coefficient in the low troposphere are mostly measured during May, while values for March and April are closer to the climatological values. This is, however, an effect of averaging over all stations. It is known that the restrictive measures were imposed at different times in Europe, therefore the effect of the lock-down (if any) has manifested at different times in the different regions. For example, in Eastern Mediterranean lower values of the aerosol backscatter coefficient were observed starting February, while in Central and Eastern Europe such decrease started in March. The amplitude is also different in various regions, being related to the intensity of the economical activity that was affected by the lock-down. April and the beginning of May seems to be uniformly characterized by lower values in the low troposphere; this is the time when restrictive measures were present in most of the regions.

The aerosol backscatter coefficient analyzed in this study is a proxy for the aerosol concentration, however a more quantitative analysis must be made to consolidate the conclusions. The values reported for the linear particle depolarization ratio show that pollen, as well as dust transported from North Africa sometime overlapped with the local aerosol. In order to conclude on the effect of the COVID-19 lock-down, further work will focus on:

- Re-analyzing the data based on large-scale circulation analogues which should provide more robust climatology than simply taking the mean of similar time periods and compare the values;
- Analyzing additional data products, such as Angstrom coefficients and lidar ratios, fine and coarse mode volume concentrations, and aerosol type; this may reveal certain changes in the aerosol composition which are not quantifiable directly from the aerosol backscatter or extinction coefficients;
- Comparing the findings with other observations such as near-surface and column measurements, passive and active sensors on board of satellites; this should bring additional information on the local influences (low PBL, where most of the lidars are “blind”) as well as regional gradients (filling the gaps between the observing stations).

Beyond the scientific goals of this analysis, the actions organized by EARLINET/ACTRIS (NRT delivery of the data and fast analysis of the data products) proved that aerosol lidars are useful for providing information not only for climatological purposes, but also in emergency situations. The stations are more and more automatic and/or remotely operated, and the centralized processing system makes the data products available very fast, at a good quality. As an example, this analysis has been done during the lock-down, when access to the lidar laboratories was very limited.

References

D'Amico, G., Amodeo, A., Baars, H., Binietoglou, I., Freudenthaler, V., Mattis, I., Wandinger, U., and Pappalardo, G.: EARLINET Single Calculus Chain – overview on methodology and strategy, Atmos. Meas. Tech., 8, 4891-4916, doi:10.5194/amt-8-4891-2015, 2015

D'Amico, G., Amodeo, A., Mattis, I., Freudenthaler, V., and Pappalardo, G.: EARLINET Single Calculus Chain – technical – Part 1: Pre-processing of raw lidar data, Atmos. Meas. Tech., 9, 491-507, doi:10.5194/amt-9-491-2016, 2016

Mattis, I., D'Amico, G., Baars, H., Amodeo, A., Madonna, F., and Iarlori, M.: EARLINET Single Calculus Chain – technical – Part 2: Calculation of optical products, Atmos. Meas. Tech., 9, 3009-3029, doi:10.5194/amt-9-3009-2016, 2016

Pappalardo, G., Amodeo, A., Apituley, A., Comeron, A., Freudenthaler, V., Linné, H., Ansmann, A., Bösenberg, J., D'Amico, G., Mattis, I., Mona, L., Wandinger, U., Amiridis, V., Alados-Arboledas, L., Nicolae, D., and Wiegner, M.: EARLINET: towards an advanced sustainable European aerosol lidar network, Atmos. Meas. Tech., 7, 2389–2409, https://doi.org/10.5194/amt-7-2389-2014, 2014.

EARLINET All 2000-2015. World Data Center for Climate (WDCC) at DKRZ. https://doi.org/10.1594/WDCC/EARLINET_All_2000-2015, 2018.